

Entanglement dynamics in double Jaynes-Cummings model and intensity-dependent double Jaynes-Cummings model for squeezed coherent thermal states

Koushik Mandal ^{*1}

¹ *Department of Physics, Indian Institute of Technology Madras, Chennai, India, 600036*

Abstract

In this work, the entanglement dynamics of different subsystems such as atom-atom, atom-field and field-field with radiation field in squeezed coherent thermal states for the intensity-dependent double Jaynes-Cummings model (IDDJCM) and double Jaynes-Cummings model (DJCM) are investigated. The effects of both squeezed photons and thermal photons on entanglement dynamics is observed. The main feature of the double Jaynes-Cummings model - entanglement sudden death is observed for every subsystem. The effects of various interactions such as Ising interaction, single photon exchange interaction and dipole-dipole interaction on entanglement dynamics are studied. The effects of detuning, Kerr-nonlinearity on the entanglement dynamics are investigated for every subsystem. It is noticed that proper choice of the interactions parameters, detuning and Kerr-nonlinearity effectively removes entanglement deaths from the dynamics.

Keywords— Double Jaynes-Cummings model, intensity-dependent double Jaynes-Cummings model, entanglement sudden death, Ising interaction, Kerr-nonlinearity, photon exchange interaction, dipole-dipole interaction, detuning.

1 Introduction

It is well known that the Jaynes-Cummings (JC) model is one of the most successful models to describe the atom-field interaction and to study the dynamics of various quantum optical quantities. Entanglement [1] is one of the important quantities which can be investigated using the Jaynes-Cummings model. In recent years, entanglement has become a ubiquitous and necessary for quantum applications. It has become a resource for quantum teleportation [2], super dense coding [3], entanglement swapping, cryptography etc. In many quantum optical systems such as in ion traps [4–7], cavity quantum electrodynamics (CQED) [8–15], circuit quantum electrodynamics [16,17] etc. entanglement is studied. All these physical systems are a mixture of atoms and fields. Jaynes-Cummings model provides a platform to study entanglements in these systems.

One of the successful extension of the usual Jaynes-Cummings model is the double Jaynes-Cummings model (DJCM). The double Jaynes-Cummings model was first introduced by Eberly [18–26]. This model can be used to study the properties of entanglement in a more extended quantum optical systems which are mentioned before. One of most striking features of the DJCM is the sudden disappearance or death of entanglement for a certain duration. This phenomena of disappearance of entanglement is termed as entanglement sudden death (ESD). After Eberly’s work, people have studied various systems with this model in various forms [27–30]. In particular in Ref. [29], the authors study entanglement dynamics of the coherent and squeezed vacuum states and the atoms. They show that the factors such as atomic spontaneous decay rate, cavity decay rate and detuning have significant effects on the entanglement

^{*}Corresponding author’s email: mandalkoushik1993@gmail.com

sudden death. To study the effects of interaction the authors in Ref. [28, 31] considered cavities with Ising type and photon exchange interactions between the cavities. The notable features of entanglement decay, sudden rebirth and sudden death have been investigated in the presence of intrinsic decoherence have been studied in Ref. [32]. In another work, Laha [33] has considered a double Jaynes-Cummings model to investigate the role of a beam-splitter, dipole-dipole interaction as well as Ising type interactions. The photonic modes in this work are considered to be either the photonic vacuum state, or the coherent states or the thermal states and the entanglements investigated are the qubit-qubit and the oscillator-oscillator type.

Another important successful generalizations of the standard Jaynes-Cummings model is the intensity-dependent Jaynes-Cummings model (IDJCM) [34, 35] which Buck and Sukumar introduced. It is also known as the Buck-Sukumar model. There are various studies done using this Hamiltonian. In [36], Buzek finds that in the intensity-dependent coupling Jaynes-Cummings model with the coherent field, light-squeezing exhibits periodic revivals. He also investigates the influence of the initial state of an atom on the squeezing of light in detail. In [37], Buzek showed that IDJCM interacting with the Holstein-Primakoff $SU(1,1)$ coherent state, the revivals of the radiation squeezing are strictly periodical for any value of the initial squeezing. He also found the expression for the atomic inversion exhibiting the exact periodicity of the population revivals. The spectrum of emitted light by a single atom interacting with a single mode radiation field in an ideal cavity via the intensity-dependent coupling was also studied by Buzek [38]. In [39], the authors have shown that in the absence of the rotating wave approximation (RWA), the J-C Hamiltonian can be transformed into an intensity-dependent Hamiltonian. They study the effects of the counter-rotating terms which appear in the intensity-dependent Hamiltonian on atomic inversion, atomic dipole squeezing, atomic entropy squeezing, photon counting statistics, field entropy squeezing etc. In another paper [40], Naderi *et al.*, has provided a theoretical scheme for the generation of nonlinear coherent states under a micromaser under an intensity-dependent J-C model. C. F. Lo *et al.*, [41] have investigated the eigenenergy spectrum of the k -photon intensity-dependent J-C model without rotating wave approximations. They show that for $k \geq 2$ the k -photon intensity dependent J-C model without RWA does not have eigenstates in the Hilbert space spanned by the photon number states, i.e., the model becomes ill-defined. K.M. Ng *et al.*, [42] also investigated the eigenenergy spectrum of the IDJCM without rotating-wave approximation. Their analysis indicated that counter-rotating terms in the Hamiltonian dramatically change the RWA energy spectrum and that the non-RWA spectrum can be approximated by the RWA spectrum only in the range of a sufficiently small coupling constant. They also showed that IDJCM without RWA is well-defined only if the coupling parameter is below a certain critical value.

Although after Eberly's work on double Jaynes-Cummings model and the entanglement sudden death, various systems with double Jaynes-Cummings model have been studied; however, there are very few studies on the intensity-dependent double Jaynes-Cummings model (IDDJCM). In [43] Xie Qin and Fang Mao-Fa have investigated the entanglement dynamics of intensity-dependent double Jaynes-Cummings model (IDDJCM) with two different initial radiation fields. One is a coherent state and another is a squeezed vacuum state. Motivated by these works, in this paper, we study the entanglement dynamics for both double Jaynes-Cummings and intensity-dependent double Jaynes-Cummings model with squeezed coherent thermal states (SCTS) and atoms in a Bell state. One of the main objectives of this work is to investigate the effects of squeezed photons and thermal photons on entanglement in a coherent background for DJCM and IDDJCM. Studying the effects of different kinds of interactions in the system is also important objective. In this paper effects of different interactions such as single photon exchange interaction, Ising interaction and dipole-dipole interaction on entanglement are investigated. We also investigate the effects of detuning, Kerr-nonlinearity [44–55] etc. Earlier, in ref. [56], the authors have studied the effects of the squeezed and thermal photons on entanglements in Jaynes-Cummings model. Here it is shown how the tussling between “classical noise” (thermal photons) and “quantum noise” (squeezed photons) affects the quantum optical properties of the radiation field, atomic inversion and entanglement dynamics for Jaynes-Cummings model. So, in this sense, our this work is a natural extension of our previous work to investigate the effects of mutual tussle between thermal and squeezed photons on entanglement dynamics of various subsystems in DJCM and IDDJCM.

The paper is organized as follows: in section 2, the double Jaynes-Cummings (DJCM) and intensity-dependent double Jaynes-Cummings model (IDDJCM) are described. Section 3 shows the entanglement dynamics for DJCM and IDDJCM. The effects of photon exchange interaction are studied in section 4. In section 5, effects of Kerr-nonlinearity are investigated. Next, the effects of Ising interaction is studied in section 6. The effects of detuning are dealt with in section 7. Section 8 deals with the effects of dipole-dipole interaction. Finally, in section 9, we conclude our results.

2 Theory

2.1 Photonic state

Squeezed coherent thermal states (SCTS) are mixed states because of the of thermal photons. The density operator for SCTS is defined as [57–59]

$$\hat{\rho}_{\text{SCT}} = \hat{D}(\alpha) \hat{S}(\zeta) \hat{\rho}_{\text{th}} \hat{S}^\dagger(\zeta) \hat{D}^\dagger(\alpha), \quad (1)$$

where

$$\hat{D}(\alpha) = \exp(\alpha \hat{a}^\dagger - \alpha^* \hat{a}) \quad (2)$$

is the displacement operator, for α a complex parameter; \hat{a} and \hat{a}^\dagger are the photon annihilation and creation operators respectively and

$$\hat{S}(\zeta) = \exp\left(-\frac{1}{2}\zeta \hat{a}^{\dagger 2} + \frac{1}{2}\zeta^* \hat{a}^2\right) \quad (3)$$

is the squeezing operator with $\zeta = r e^{i\varphi}$; where ζ is the squeezing parameter; r and φ denote the amplitude and phase of ζ respectively. The density operator of a thermal radiation field with a heat bath at temperature T can be written as

$$\hat{\rho}_{\text{th}} = \frac{1}{1 + N_{th}} \sum_{n=0}^{\infty} \left(\frac{N_{th}}{N_{th} + 1}\right)^n |n\rangle \langle n|, \quad (4)$$

where N_{th} is the average number of thermal photons and it is given by

$$N_{th} = \frac{1}{\exp\left(\frac{h\nu}{k_B T}\right) - 1}; \quad (5)$$

k_B is Boltzmann constant and ν is linear frequency of radiation field in Eq. 5. The analytic expression for the PCD of SCTS can be written as [57, 58]

$$P(l) = \langle l | \hat{\rho}_{\text{SCT}} | l \rangle \quad (6)$$

$$= \pi Q(0) \tilde{A}^l \sum_{q=0}^l \frac{1}{q!} \left(\frac{l}{q}\right) \left|\frac{\tilde{B}}{2\tilde{A}}\right|^q \times |H_q((2B)^{-1/2} \tilde{C})|^2, \quad (7)$$

where $\pi Q(0) = R(0, 0)$; R is Glauber's R -function [60];

$$R(0, 0) = [(1 + A)^2 - |B|^2]^{-1/2} \exp\left\{-\frac{(1 + A)|C|^2 + \frac{1}{2}[B(C^*)^2 + B^* C^2]}{(1 + A)^2 - |B|^2}\right\}, \quad (8)$$

where

$$A = N_{th} + (2N_{th} + 1)(\sinh r)^2, \quad (9)$$

$$B = -(2N_{th} + 1)e^{i\varphi} \sinh r \cosh r, \quad (10)$$

$$C = \alpha \quad (\text{for SCTS}), \quad (11)$$

$$C = \alpha \cosh r + \alpha^* e^{i\varphi} \sinh r, \quad (\text{for CSTS}) \quad (12)$$

and

$$\tilde{A} = \frac{A(1 + A) - |B|^2}{(1 + A)^2 - |B|^2}, \quad (13)$$

$$\tilde{B} = \frac{B}{(1 + A)^2 - |B|^2}, \quad (14)$$

$$\tilde{C} = \frac{(1 + A)C + B C^*}{(1 + A)^2 - |B|^2}. \quad (15)$$

If we write \tilde{A} , \tilde{B} and \tilde{C} in terms of N_{th} and r , we get

$$\tilde{A} = \frac{N_{th}(N_{th} + 1)}{N_{th}^2 + (N_{th} + \frac{1}{2})[1 + \cosh(2r)]} \quad (16)$$

$$\tilde{B} = -\frac{e^{i\varphi}(N_{th} + \frac{1}{2}) \sinh(2r)}{N_{th}^2 + (N_{th} + \frac{1}{2})[1 + \cosh(2r)]} \quad (17)$$

$$\tilde{C} = \frac{C[\frac{1}{2} + (N_{th} + \frac{1}{2}) \cosh r] - C^* e^{i\varphi}(N_{th} + \frac{1}{2}) \sinh 2r}{N_{th}^2 + (N_{th} + \frac{1}{2})[1 + \cosh(2r)]} \quad (18)$$

and H_q is the Hermite polynomial. It is defined as

$$H_q(x) = \sum_{j=0}^{\lfloor \frac{q}{2} \rfloor} \frac{(-1)^j q!}{j!(q-2j)!} (2x)^{q-2j}. \quad (19)$$

2.2 Atomic state

In the double Jaynes-Cummings model, there are two two-level atoms, one in cavity a and the other in cavity b, respectively. These two-level systems are initially prepared in either as a pure state or as a mixed state. For the pure state a maximally entangled Bell state is considered. In this paper, we use the entangled state of the form

$$|\psi\rangle_{AB} = \cos \theta |e_A, g_B\rangle + \sin \theta |g_A, e_B\rangle, \quad (20)$$

where $|e_A\rangle$, $|e_B\rangle$ and $|g_A\rangle$, $|g_B\rangle$ correspond to the excited and ground states of the atom A and atom B respectively.

2.3 The Hamiltonian of the system

Now, we introduce the Hamiltonian for IDDJCM which is given by

$$\begin{aligned} \hat{H} = & \omega \hat{\sigma}_z^A + \omega \hat{\sigma}_z^B + \nu \hat{a}^\dagger \hat{a} + \nu \hat{b}^\dagger \hat{b} + \lambda \left(\sqrt{\hat{N}_a} \hat{a}^\dagger \hat{\sigma}_-^A + \hat{a} \sqrt{\hat{N}_a} \hat{\sigma}_+^A \right) \\ & + \lambda \left(\sqrt{\hat{N}_b} \hat{b}^\dagger \hat{\sigma}_-^B + \hat{b} \sqrt{\hat{N}_b} \hat{\sigma}_+^B \right). \end{aligned} \quad (21)$$

The factor $\hat{\sigma}_z^i$ represents the Pauli matrix in the z -basis and $\hat{\sigma}_+^i$ and $\hat{\sigma}_-^i$ are the spin raising and lowering operators respectively. The index i represents the atomic label. The photonic operators \hat{a} and \hat{b} are the annihilation operators corresponding to the two different cavities and the operators \hat{a}^\dagger and \hat{b}^\dagger are the corresponding creation operators. The coupling constant is represented by λ and it describes the strength of the atom-field interaction with ω and ν being the atomic transition frequency and the radiation frequency respectively. \hat{N}_a and \hat{N}_b are the number operators for fields in cavities a and b respectively. For $\hat{N}_a = 1$ and $\hat{N}_b = 1$, we get the usual Hamiltonian for DJCM

$$\hat{H}' = \omega \hat{\sigma}_z^A + \omega \hat{\sigma}_z^B + \nu \hat{a}^\dagger \hat{a} + \nu \hat{b}^\dagger \hat{b} + \lambda (\hat{a}^\dagger \hat{\sigma}_-^A + \hat{a} \hat{\sigma}_+^A) + \lambda (\hat{b}^\dagger \hat{\sigma}_-^B + \hat{b} \hat{\sigma}_+^B). \quad (22)$$

The initial state vector of the atom-field system

$$|\psi(0)\rangle = |\psi\rangle_{AB} \otimes |\psi_F\rangle_a |\psi_F\rangle_b = (\cos \theta |e, g\rangle + \sin \theta |g, e\rangle) \otimes \left(\sum_{n=0}^{\infty} c_n |n\rangle \sum_{m=0}^{\infty} d_m |m\rangle \right). \quad (23)$$

The basis states for this atom-field system are $|e, g, n, m\rangle$, $|g, e, n, m\rangle$, $|g, g, n+1, m\rangle$, $|g, g, n, m-1\rangle$, $|e, e, n-1, m\rangle$, $|e, e, n, m-1\rangle$, $|g, e, n+1, m-1\rangle$, $|e, g, n-1, m+1\rangle$. To get the $\psi(t)$ we need to solve the Schrodinger equation for IDDJCM and DJCM. For this purpose let us solve the single Jaynes-Cummings models first. Let the initial state of the atom-field system in the single J-C model be

$$|\psi_I(0)\rangle = |e\rangle \otimes |n\rangle. \quad (24)$$

After time evolution under the single Jaynes-Cummings Hamiltonian, the state becomes

$$|\psi_I(t)\rangle = x_1(t) |e\rangle |n\rangle + x_2(t) |g\rangle |n+1\rangle, \quad (25)$$

where $x_1(t)$ and $x_2(t)$ are the probability amplitudes for the system to be found in $|e\rangle |n\rangle$ and $|g\rangle |n+1\rangle$ states respectively. After solving the Schrödinger equation for this state with the initial conditions $x_1(0) = 1$ and $x_2(0) = 0$, we get

$$x_1(t) = \cos(\lambda\sqrt{n+1}t), \quad (26)$$

$$x_2(t) = -i \sin(\lambda\sqrt{n+1}t). \quad (27)$$

For intensity-dependent single J-C Hamiltonian

$$x_1(t) = \cos(\lambda(n+1)t), \quad (28)$$

$$x_2(t) = -i \sin(\lambda(n+1)t). \quad (29)$$

If the system starts from

$$|\psi_I(0)\rangle = |g\rangle \otimes |n\rangle, \quad (30)$$

then after evolution, the state becomes

$$|\psi_I(t)\rangle = y_1(t) |g\rangle |n\rangle + y_2(t) |e\rangle |n-1\rangle. \quad (31)$$

As before, solving for the initial conditions $y_1(0) = 1$ and $y_2(0) = 0$, we get

$$y_1(t) = \cos(\lambda\sqrt{n}t), \quad (32)$$

and

$$y_2(t) = -i \sin(\lambda\sqrt{n}t). \quad (33)$$

In the intensity-dependent case

$$y_1(t) = \cos(\lambda n t), \quad (34)$$

and

$$y_2(t) = -i \sin(\lambda n t). \quad (35)$$

In the double Jaynes-Cummings model, the initial state for the atom-field system is

$$|\psi(0)\rangle = |\psi\rangle_{AB} \otimes |\psi_F\rangle_a |\psi_F\rangle_b = (\cos\theta |e, g\rangle + \sin\theta |g, e\rangle) \otimes \left(\sum_{n=0}^{\infty} c_n |n\rangle \sum_{m=0}^{\infty} d_m |m\rangle \right), \quad (36)$$

where we consider the atomic states corresponding to the cavities a and b are entangled. So, after time evolution the initial state in Eq. (36) evolves to

$$\begin{aligned} |\psi(t)\rangle &= \cos\theta \sum_n c_n (x_1(t) |e, n\rangle + x_2(t) |g, n+1\rangle) \otimes \sum_m d_m (y_1(t) |g, m\rangle + y_2(t) |e, m-1\rangle) \\ &\quad + \sin\theta \sum_n c_n (x_1(t) |e, n\rangle + x_2(t) |g, n+1\rangle) \otimes \sum_m d_m (y_1(t) |g, m\rangle + y_2(t) |e, m-1\rangle), \end{aligned} \quad (37)$$

which can be rewritten as

$$\begin{aligned} |\psi(t)\rangle &= \sum_{n,m=0}^{\infty} a_1(n, m, t) |e, g, n, m\rangle + a_2(n, m, t) |e, e, n, m-1\rangle + a_3(n, m, t) |g, g, n+1, m\rangle \\ &\quad + a_4(n, m, t) |g, e, n+1, m-1\rangle + a_5(n, m, t) |g, e, n, m\rangle + a_6(n, m, t) |g, g, n, m+1\rangle \\ &\quad + a_7(n, m, t) |e, e, n-1, m\rangle + a_8(n, m, t) |e, g, n-1, m+1\rangle, \end{aligned} \quad (38)$$

where the factors a_i 's are as given below:

$$\begin{aligned}
a_1(n, m, t) &= \cos \theta \sum_n c_n x_1(t) \sum_m d_m y_1(t); & a_2(n, m, t) &= \cos \theta \sum_n c_n x_2(t) \sum_m d_m y_2(t); \\
a_3(n, m, t) &= \cos \theta \sum_n c_n x_2(t) \sum_m d_m y_1(t); & a_4(n, m, t) &= \cos \theta \sum_n c_n x_2(t) \sum_m d_m y_2(t); \\
a_5(n, m, t) &= \sin \theta \sum_n c_n y_1(t) \sum_m d_m x_1(t); & a_6(n, m, t) &= \sin \theta \sum_n c_n y_1(t) \sum_m d_m x_2(t); \\
a_7(n, m, t) &= \sin \theta \sum_n c_n y_2(t) \sum_m d_m x_1(t); & a_8(n, m, t) &= \sin \theta \sum_n c_n y_2(t) \sum_m d_m x_2(t).
\end{aligned}$$

From the knowledge of the time evolved state, one can construct the time evolved density matrix $\rho(t)$ which can be used to calculate the entanglement between different subsystems like the atom-atom, the atom-field and the field-field subsystems.

2.4 Entanglement measures

To characterize the dynamics of entanglement, we need to measure the entanglement in the system. In our work we investigate the dynamics of the bipartite entanglements like the atom-atom entanglement, atom-field entanglement and the field-field entanglement. The atom-atom entanglement can be conclusively measured using concurrence defined in [61]

$$C_{AB} = \max\{0, \xi_1 - \xi_2 - \xi_3 - \xi_4\}, \quad (39)$$

where $\xi_i (i = 1, 2, 3, 4)$ are the decreasingly ordered square roots of the eigenvalues of the matrix $\hat{\rho}(\hat{\sigma}_y^A \otimes \hat{\sigma}_y^B) \hat{\rho}^* (\hat{\sigma}_y^A \otimes \hat{\sigma}_y^B)$ and $\hat{\rho}$ is the two qubit atom-atom reduced density matrix. The value of concurrence lies in the range $0 \leq C \leq 1$, where $C = 0$ implies a separable state and $C = 1$ denotes a maximally entangled state. Though concurrence can be used to compute entanglement in both pure and mixed states, it works only for $2 \otimes 2$ systems, so for higher dimensional systems we need to use other measures. In particular, when we consider the atom-field and field-field subsystems we are looking at $2 \otimes \infty$ and bipartite continuous variable systems. For these systems it is convenient to use the negativity [62] which is defined as

$$N(t) = \sum_k \left(|\xi_k| - \xi_k \right) / 2, \quad (40)$$

where ξ_k are the eigenvalues of $\hat{\rho}^{PT}$, the partial transpose of the density matrix, i.e., the matrix which is transposed with respect to any one of the subsystems.

3 Entanglement dynamics in IDDJCM and DJCM

In this section, we study the entanglement dynamics of the atom-field system with radiation field in SCTS with atoms in a Bell state. Fig. 1 represents the entanglement dynamics for IDDJCM. To study the dynamics, $\bar{n}_c = 2$, $\bar{n}_{th} = 1.0$ and $\bar{n}_s = 0.1, 0.3, 0.5, 1.0$ have been taken. It is already shown in earlier studies of the intensity-dependent Jaynes-Cummings model that the dynamics of the system show a periodic nature [43]. From Fig. 1, it is observed that $C(t)$ for the atom-atom subsystem and $N(t)$ for all the other three subsystems show periodic dynamics. From Fig. 1(a), we notice that the dynamics of $C(t)$ does not change considerably with increasing squeezed photons. Lengths of the ESDs in the dynamics change very little with the increment in \bar{n}_s and the heights of the peaks do not change at all. This is also exactly the same for the field-field subsystem in Fig. 1(d). For atom A-field a subsystem in Fig. 1(b), the amplitude of $N(t)$ increases keeping the shape of the dynamics almost similar; however, there is no change in ESDs. In Fig. 1(c), for atom A-field b subsystem, peak heights decrease and lengths of ESDs also decrease with increasing \bar{n}_s . So, for field-field subsystem, increase in number of squeezed photons does not affect the $C(t)$ and $N(t)$. The dynamics almost superimpose on one another. Fig. 2 shows how the entanglement is shared with time between different subsystems for a fixed \bar{n}_s .

In Fig. 3, the entanglement dynamics for DJCM are plotted. The dynamics are very different from the dynamics obtained in IDDJCM. The periodic nature of entanglement (like periodic pulse) is not observed for DJCM. In the case of atom-atom entanglement, $C(t)$ starts from highest value and then falls very sharply. $C(t)$ shows a large ESD and the duration of ESD increases with increasing value of \bar{n}_s .

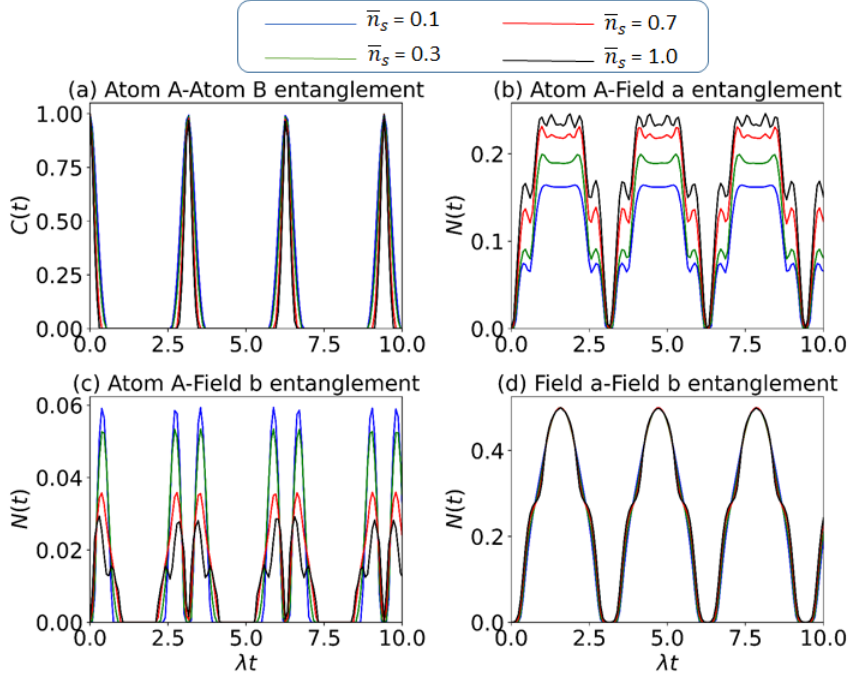


Figure 1: Entanglement dynamics for atom A-atom B, atom A-field a, atom a-field b and field a-field b with atoms in a Bell state and field in SCTS for IDDJCM. The values of the parameters used in these plots are $\bar{n}_c = 2$, $\bar{n}_{th} = 0.1$, $\bar{n}_s = 0.1, 0.3, 0.5, 1.0$ and $\theta = \frac{\pi}{4}$.

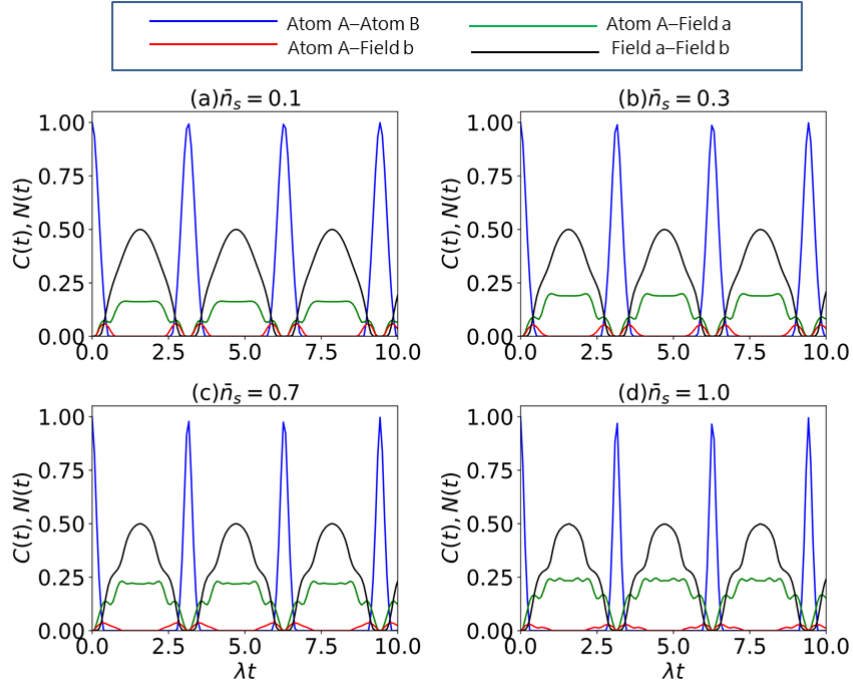


Figure 2: All the entanglements in Figure 1 are plotted in a single plot for various n_s .

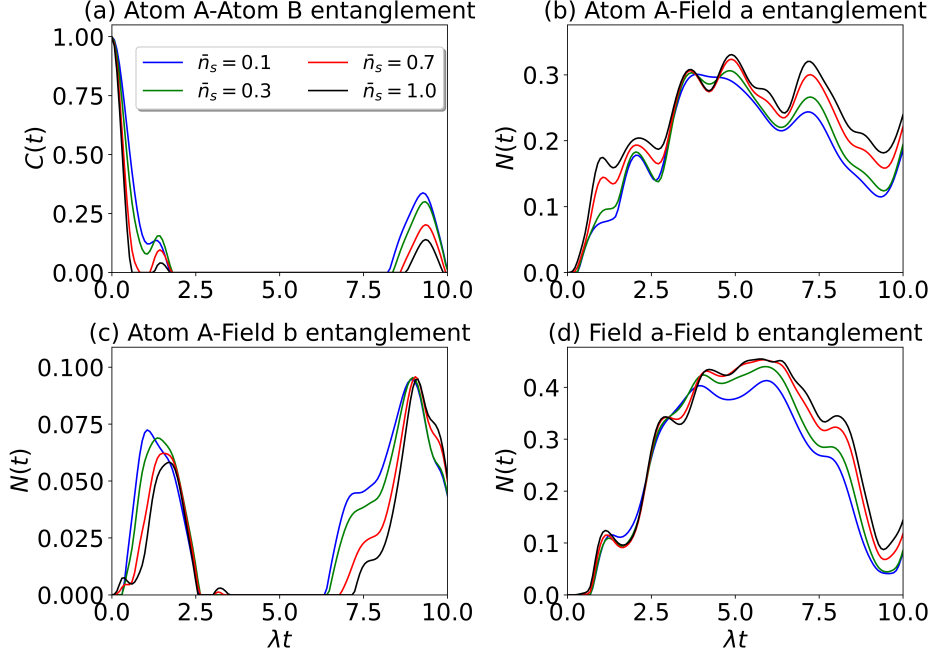


Figure 3: Entanglement dynamics for atom A-atom B, atom A-field a, atom a-field b and field a-field b with atoms in a Bell state and field in SCTS for DJCM. The values of the parameters used in these plots are $\bar{n}_c = 2$, $\bar{n}_{th} = 0.1$, $\bar{n}_s = 0.1, 0.3, 0.5, 1.0$ and $\theta = \frac{\pi}{4}$.

The effects of thermal photons are also visible here. In the case of squeezed coherent state [57–59, 63–73], smaller peaks were present in the dynamics of $C(t)$ and the height of the peaks $\lambda t = 8$ were bigger. Those smaller peaks disappear and the heights of the aforementioned peaks also come down. In a sense, the thermal photons destroys the entanglement in atom-atom subsystem.

3.1 Wigner function distributions for SCTS

Before, to proceed further in this paper to investigate the effects of different interactions, we discuss the Wigner function $W(\alpha)$ for SCTS in IDDJCM and DJCM. Wigner function distributions are of major importance in quantum optics. $W(\alpha)$ is defined as [74–76]

$$W(\alpha) = \frac{1}{\pi^2} \int d^2\beta \text{Tr}[\hat{\rho}\hat{D}(\beta)] \exp(\beta^*\alpha - \beta\alpha^*). \quad (41)$$

The density operator $\hat{\rho}$ for SCTS is given in Eq. (1).

Wigner functions $W(\alpha)$ for SCTS in IDDJCM are depicted in Fig. 4. In these plots $\bar{n}_c = 2.0$, $\bar{n}_s = 0.1$ and $\bar{n}_{th} = 0.1$ are chosen. It is observed that at $t = 0$, $W(\alpha)$ is positive and it is a shifted Gaussian; however, at $t = 2$ s the peak of $W(\alpha)$ decreases significantly and at some region it becomes negative. The negative peak is almost 30% of the peak at $t = 2$ s. After that, the negativity of $W(\alpha)$ decreases and at $t = 6$ s, it almost resembles the initial peak at $t = 0$ s. As time increases further, it is noticed that negativity of Wigner function increases again at $t = 8$ s and again it decreases. So, it is observed that $W(\alpha)$ changing value from positive to negative and vice versa as time progresses. It indicates that the state of radiation oscillating between a classical state and non-classical state as an effect of atom-field interaction in IDDJCM.

Figure 5 represents the Wigner function distributions for SCTS in DJCM. In this case also, $W(\alpha)$ starts from a shifted Gaussian shape at $t = 0$ s. At $t = 2$ s its positive peak comes down very drastically and in some region it becomes negative (almost 50%) of the highest of value. As time increases, the shape of $W(\alpha)$ changes and negative values decreases. However, it is contrasting compared to the case with IDDJCM that $W(\alpha)$ does not become positive again and mimic the initial state. The Wigner function for SCTS shows negative values for a longer period of time in DJCM. It shows that SCTS become more non-classical as a result of atom-field interaction in DJCM as compared to the case in IDDJCM.

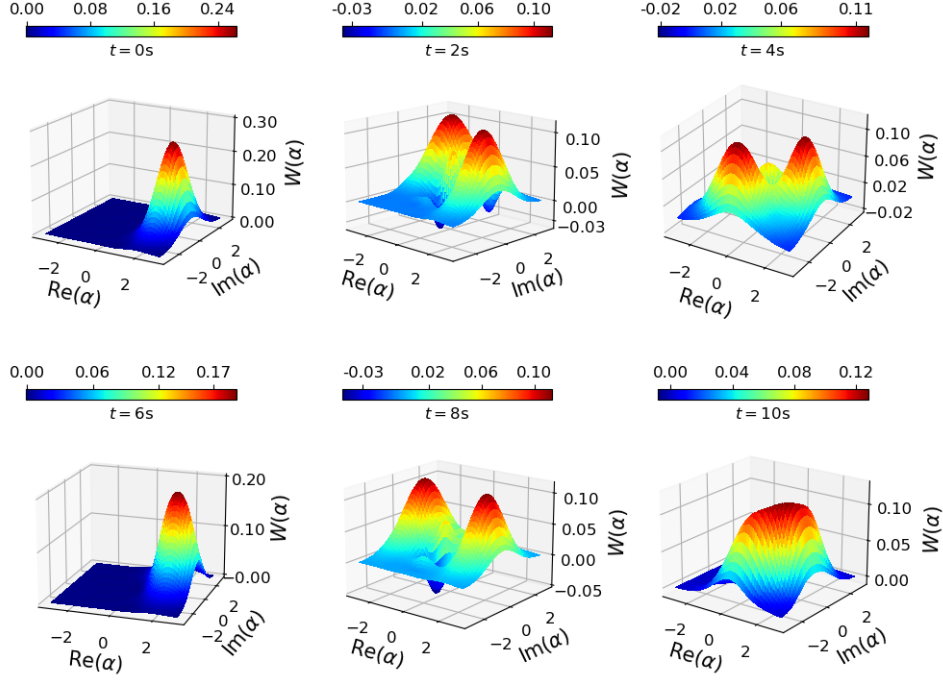


Figure 4: Wigner functions for SCTS in IDDJCM. The values of the parameters used in here are $\bar{n}_c = 2.0$, $\bar{n}_s = 0.1$, $\bar{n}_{th} = 0.1$ and $\theta = \frac{\pi}{4}$.

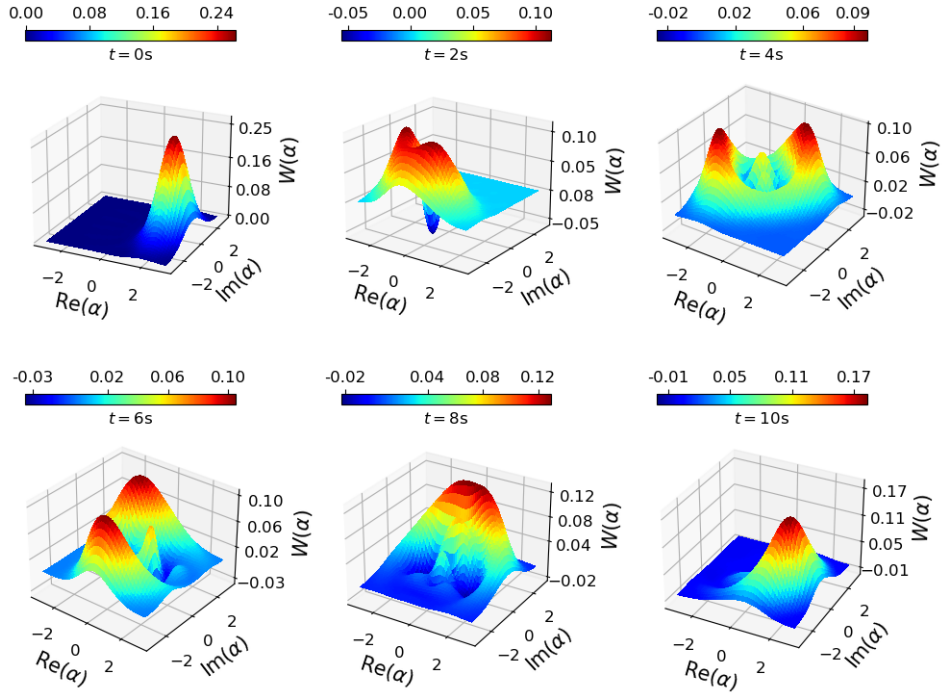


Figure 5: Wigner functions for SCTS in DJCM. The values of the parameters used in here are $\bar{n}_c = 2.0$, $\bar{n}_s = 0.1$, $\bar{n}_{th} = 0.1$ and $\theta = \frac{\pi}{4}$.

4 Effects of single photon exchange interaction on the entanglement dynamics of the atom-field system

Now we study the effects of single photon exchange between the two cavities on entanglement dynamics. Recently, people have been studying systems in which photons can hop from one atom-cavity system to another. Pandit *et. al.*, [28,31] have studied the effects of cavity-cavity interaction on the entanglement dynamics of a generalized double Jaynes-Cummings model. The authors have shown that for larger value of κ , entanglement for the atom-atom subsystem can be protected. They have also investigated the role of κ in entanglement transfer between atom-atom and field-field subsystems. In another work, Laha [33] has investigated the effects of beam-splitter which is equivalent to photon exchange interaction on entanglement dynamics in DJCM for radiation states in vacuum, coherent and thermal states. The effects of photon exchange interaction is modeled by the following Hamiltonian:

$$\hat{H}_{\text{PE}} = \hat{H} + \kappa \hat{a}^\dagger \hat{a} + \kappa \hat{b}^\dagger \hat{b} \quad (42)$$

where κ is the cavity-cavity photon exchange coupling term. Without intensity dependence this Hamiltonian becomes

$$\hat{H}'_{\text{PE}} = \hat{H}' + \kappa \hat{a}^\dagger \hat{a} + \kappa \hat{b}^\dagger \hat{b} \quad (43)$$

Figure 6 shows the effects of cavity-cavity single photon exchange interaction on the entanglement dynamics for SCTS in IDDJCM. The strength of this cavity-cavity interaction via single photon exchange is characterized by the parameter κ . To study the effects of κ , $\bar{n}_c = 2$, $\bar{n}_s = 1$ and $\bar{n}_{th} = 0.1$ are taken. From Fig. 6(a) it is observed that for $\kappa = 0.1$ i.e., $\kappa < \lambda$, the peak of atom A-atom B entanglement pulses decreases with time (described by blue curve), however, the lengths of ESDs do not change considerably. The field a-field b entanglement which is represented by the black curve shows different behaviour. If we compare Figs. 6(d) and 1(d), it can be seen that ESDs are removed from the dynamics and the amplitude of $N(t)$ increases with time. For both atom A-field a (green curve) and atom A-field b (red curve), the periodic nature of $N(t)$ gets destroyed however the amplitude of $N(t)$ does not change noticeably. For $\kappa = \lambda$ ($\kappa = 1$), peaks of $C(t)$ decreases rapidly with time, it is also observed that the length of the first ESD increases however the length of other ESDs decreases at some places. For field-field entanglement, the amplitude of $N(t)$ rises up sharply and then it becomes oscillatory. For the atom A-field a and atom A-field b, all the ESDs are removed from the dynamics though the amplitude of $N(t)$ in these subsystems are small. As we increase κ further i.e., $\kappa > \lambda$ ($\kappa = 5$), it is observed that ESD in the dynamics of $C(t)$ are removed initially and many smaller peaks appear in the dynamics. From the plot, it is evident that this photon exchange interaction is creating atom-atom entanglement in the system. In the field-field entanglement, $N(t)$ shows reduction in its amplitude which can be explained as the increase on number of smaller peaks and disappearance of ESDs in $C(t)$; entanglement is transferred from $N(t)$ to $C(t)$. Also, the frequency of field-field entanglement increases significantly. The atom A-field a entanglement is decreased and it almost becomes zero at some places. $N(t)$ for atom A-field b does not change considerably, however it becomes zero when atom-atom and field-field entanglement are maximum. As we increase the value of κ to 10, we have a situation where $\kappa \gg \lambda$ i.e., photon exchange coupling between the cavities is more powerful than coupling between the atoms and radiation field. All the ESDs from the dynamics of $C(t)$ is removed and the value of $C(t)$ increases by a large amount. This increase in atom-atom entanglement makes the field-field entanglement to decrease considerably; entanglement is transferred from field-field subsystem to atom-atom subsystem. $N(t)$ for atom A-field a and atom A-field b are almost zero everywhere except some very little peaks initially. So, we observe that for large photon exchange coupling between the cavities ESDs are removed from atom-atom dynamics and also the amplitude increases significantly. $N(t)$ for field-field entanglement too gets rid of ESDs with the addition of κ in the system; however, its amplitude decreases with increasing value of κ .

Figure 7 shows the effects of photon exchange interaction for SCTS in DJCM. The maximum value of $N(t)$ for field-field subsystem increases by almost three times as a result of photon exchange interaction. For $\kappa = 0.1$, which is a low value compared to the atom-field coupling constant λ . For this low value of κ , the lengths of ESD for atom-atom entanglement increase and other smaller peaks disappear. The atom A-field a entanglement comes down significantly and at some places $N(t)$ almost becomes zero. In the case of the atom A-field b entanglement, we observed that the ESDs are removed from the dynamics of $N(t)$. For $\kappa = 1.0$, the length of ESD of $C(t)$ becomes larger as small peaks disappear. $N(t)$ for field-field entanglement increases very sharply and then comes down again. Its maximum value also decreases as compared to the case when $\kappa = 0.1$. In atom A-field a subsystem, ESD occurs as a result of increase in κ . No, considerable change is noticed in atom A-field a entanglement. As κ is increased further to

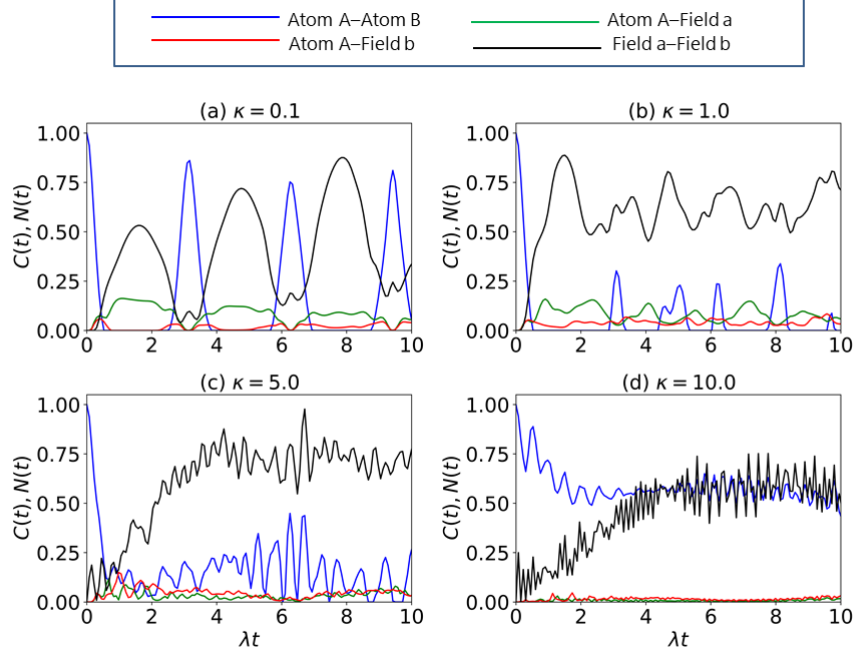


Figure 6: Effects of photon exchange interaction on entanglement dynamics for SCTS in ID-DJCM. The values of the parameters used in these plots are $\bar{n}_c = 2$, $\bar{n}_{th} = 0.1$, $\bar{n}_s = 1.0$, $\kappa = 0.1, 1.0, 5.0, 10.0$ and $\theta = \frac{\pi}{4}$.

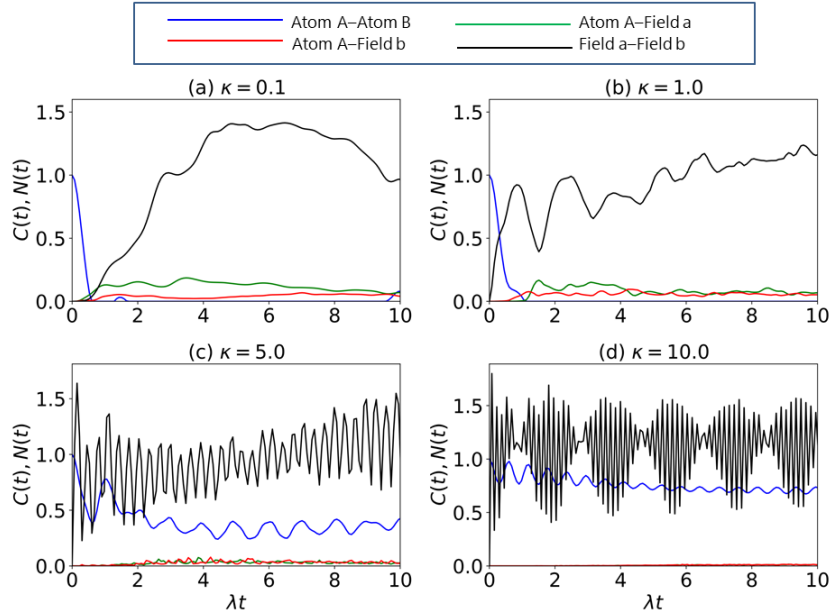


Figure 7: Effects of photon exchange interaction on entanglement dynamics for SCTS in DJCM. The values of the parameters used in these plots are $\bar{n}_c = 2$, $\bar{n}_{th} = 0.1$, $\bar{n}_s = 1.0$, $\kappa = 0.1, 1.0, 5.0, 10.0$ and $\theta = \frac{\pi}{4}$.

5, a drastic change is observed in the entanglement dynamics of $C(t)$. We see that all the ESDs are removed from the dynamics and its value also increases significantly at every instant of time. In field-field entanglement, we notice that the maximum value of $N(t)$ increases and the dynamics become very oscillatory. $N(t)$ for atom A-field a and atom A-field b shows initially and after that it stays nonzero with

very low amplitude. When $\kappa \gg \lambda$ i.e., for $\kappa = 10$, $C(t)$ increases more and remains high. We observe interesting pattern in the dynamics of $N(t)$ for field-field entanglement. In this case wave packets of entanglement are formed and amplitude of the wave packets increase significantly. $N(t)$ for atom A-field a and atom A-field b entanglements becomes zero. From this analysis we conclude that photon exchange interaction creates entanglement in the atom-atom and field-field subsystems. However, in the case of IDDJCM, we observe that $C(t)$ increases and $N(t)$ for field-field entanglement decreases; however, in the case of DJCM both $C(t)$ and $N(t)$ for the field-field entanglement increase. In both IDDJCM and DJCM, atom A-field a and atom A-field b entanglements become zero with increasing κ .

5 Effects of Kerr-nonlinearity on the entanglement dynamics in IDDJCM

In this section, the effects of Kerr-nonlinearity on entanglement dynamics for IDDJCM and DJCM are investigated. The Hamiltonian of atom-field system with Kerr-nonlinearity is

$$\hat{H}_{\text{Kerr}} = \hat{H} + \chi \hat{a}^{\dagger 2} \hat{a}^2 + \chi \hat{b}^{\dagger 2} \hat{b}^2, \quad (44)$$

$$\hat{H}'_{\text{Kerr}} = \hat{H}' + \chi \hat{a}^{\dagger 2} \hat{a}^2 + \chi \hat{b}^{\dagger 2} \hat{b}^2, \quad (45)$$

where $\chi = k\omega$ is the nonlinear coupling constant and k is a non-negative number. Studying the effects of nonlinearity in the system has drawn attention in the past and in recent years [44–53].

Kerr-nonlinearity affects the dynamics of atom-field interaction and other quantum optical quantities such as the Q-function, Wigner function [46] etc. significantly. In ref. [77], the authors have studied the effects of Kerr-nonlinearity and atom-atom coupling on the degree of atom-atom entanglement. In another work ref., [78] Thabet *et. al*, have investigated the effects of Kerr-nonlinearity on the mean photon number, Mandel's Q parameter, entropy squeezing and entanglement dynamics using nonlinear Jaynes-Cummings model. Xi-Wen Hou *et. al*, [79], have studied the dynamical properties of quantum entanglement in the integrable Jaynes-Cummings model with Kerr-nonlinearity with various Kerr coupling parameters and initial states, where the initial states are prepared by the coherent states placed in the corresponding phase space described in terms of canonical variables.

Figure 8 represents the entanglement dynamics after adding Kerr-nonlinearity. The addition of nonlinearity $\chi = 0.1$ totally destroys the periodic nature of the entanglement for all the subsystem (blue curve in the plots). ESDs from the dynamics are removed for atom A-field a, atom A-atom b and field a-field b subsystems; however in the case of atom A-atom B, there are long ESDs and short ESDs present in the system. As χ is increased to 0.3, a different behaviour is observed. ESDs get removed from the dynamics of $C(t)$ with increasing amplitude; however, for all the other subsystems the amplitude of $N(t)$ decreases (green curve). For $\chi = 0.7$, which is represented by the red curve in the plots, we observe that the amplitude of $C(t)$ increases and $N(t)$ for field a-field b increases again. For atom A-field a and atom A-field b subsystems, though $N(t)$ decreases at the beginning of the dynamics, it increases with time. So, it can be concluded there is a value χ for which $N(t)$ becomes minimum and beyond that value it increases again. As we increase the nonlinearity further to $\chi = 1.0$, all the entanglements increase with time which can be seen from the plots (black curve).

The effects of χ on entanglement dynamics of different subsystems for SCTS in DJCM are presented in Fig. 9. For $\chi = 0.1$, ESD in $C(t)$ decreases considerably with a couple of smaller peaks in the dynamics (Fig. 9(a), blue curve). $N(t)$ for the atom A-field a subsystems are reduced as a result of addition of Kerr-nonlinearity. In the atom A-field b subsystem, we notice that ESDs are removed from the dynamics of $N(t)$ for $\chi = 0.1$. In the field-field entanglement, we observe a increase in the entanglement. This increment in the atom-atom and field-field entanglement can be interpreted as the transfer of entanglement from atom A-field a subsystem and creation of entanglement by Kerr-nonlinearity. As χ is increased to 0.3, the amplitude of $C(t)$ increases very significantly, and ESDs which were present initially in the dynamics get removed. The length of ESDs also gets shortened further (green curve). For other entanglements, $N(t)$ for atom A-field a and atom A-field b decreases prominently as increasing nonlinearity in the system. However, $N(t)$ for the field a-field b subsystem increases again which is opposite as compared to the case in IDDJCM. However, the atom A-field a and atom A-field b entanglement become half of the previous value. If we look into the $N(t)$ of field-field subsystem, it can be seen that the amplitude of $N(t)$ increases remarkably. On further increasing the value of χ to 0.7 and 1.0, $C(t)$ keeps on increasing further and further with greater amplitude. This time, in the atom A-field a

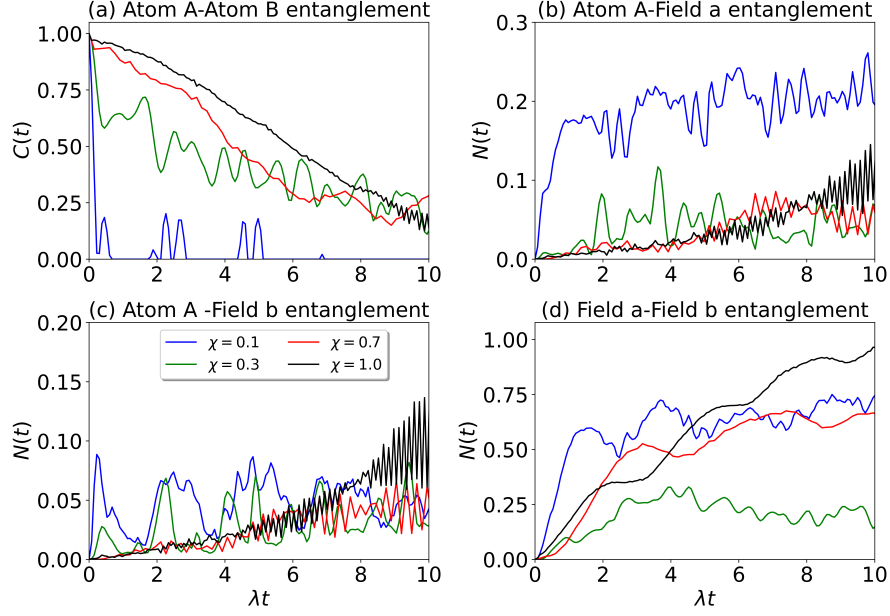


Figure 8: Effects of Kerr-nonlinearity on the entanglement dynamics for SCTS in IDDJCM with atoms in a Bell state. The values of the parameters used in these plots are $\bar{n}_c = 2$, $\bar{n}_{th} = 0.1$, $\bar{n}_s = 1.0$, $\chi = 0.1, 0.3, 0.7, 1.0$ and $\theta = \frac{\pi}{4}$.

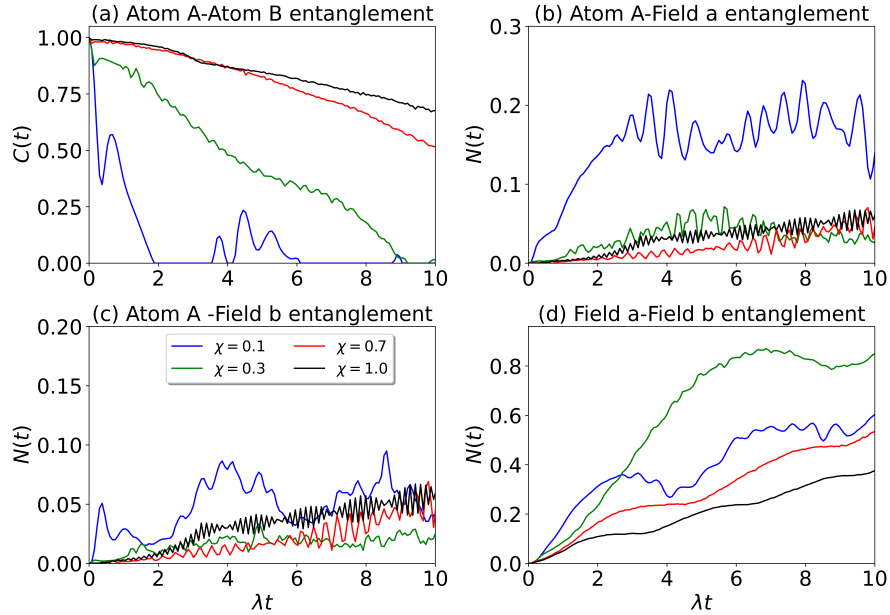


Figure 9: Effects of Kerr-nonlinearity on the entanglement dynamics for SCTS in DJCM with atoms in a Bell state. The values of the parameters used in these plots are $\bar{n}_c = 2$, $\bar{n}_{th} = 0.1$, $\bar{n}_s = 1.0$, $\chi = 0.1, 0.3, 0.7, 1.0$ and $\theta = \frac{\pi}{4}$.

and atom A-field b subsystems, $N(t)$ increases and waves packets are formed in the dynamics for $\chi = 1.0$. On the other hand, field-field entanglement decreases with these increased values. So, there is a critical value of χ for which $N(t)$ for atom A-field a and atom A-field b gets minimum and after that it increases again; also for that value field-field starts to decrease. So, for a certain range of values χ , entanglement is created in the atom-atom and field-field subsystems and transferred from the atom-field subsystems. After the critical value of χ , entanglement is created in the atom-atom and atom-field subsystems and transferred from the field-field subsystem.

6 Effects of spin-spin Ising interaction between the two atoms on entanglement dynamics

In the present section we study the effects of Ising-type interaction between the two atoms on the entanglement dynamics. The Hamiltonian with Ising-type interaction for IDDJCM and DJCM can be written as follows:

$$\hat{H}_{\text{IS}} = \hat{H} + J_z \hat{\sigma}_z^{\text{A}} \otimes \hat{\sigma}_z^{\text{B}}, \quad (46)$$

and

$$\hat{H}'_{\text{IS}} = \hat{H}' + J_z \hat{\sigma}_z^{\text{A}} \otimes \hat{\sigma}_z^{\text{B}}, \quad (47)$$

where J_z is the coupling strength between the two atoms. J_z has the unit of energy. Recently people have studied the Ising-type interaction for different configurations. Ghoshal *et. al.*, have investigated the entanglement dynamics of the quenched disordered double Jayens-Cummings model in the presence of Ising-type interaction in the Hamiltonian [31]. In another work, Pandit *et. al.*, have also studied the effects of Ising-type interaction on the entanglement dynamics in the DJCM [28]. In ref. [33] has analyzed the effects of Ising-type interaction on entanglement in DJCM for vacuum, coherent and thermal states of radiation fields. Sadiq *et. al.*, [80] have investigated the time evolution and asymptotic behaviour of entanglement with considering the dipole-dipole and Ising-type interactions in the Hamiltonian.

The effects of Ising interaction on entanglement for IDDJCM are shown in Fig. 10. The plots show very different effects as is observed in DJCM for SCS and G-L states. From Figs. 10(a) and 10(b), it can be seen that for $J_z = 0.1$ and 0.3 , we cannot distinguish the plots from the plots with $J_z = 0$ for $C(t)$ and $N(t)$ (see Figs. 1 and 10). However, for atom A-field b entanglement, the amplitude of $N(t)$ comes down and ESDs are also present in the dynamics. In the case of field a-field b entanglement, for the above mentioned values of J_z , we observe that ESDs are removed from the dynamics and amplitude increases. For $J_z = 0.7$, small peaks appear along with the large peaks in the dynamics of $C(t)$ (red curve) and also the amplitude decreases. For atom A-field a subsystem, the amplitude of $N(t)$ comes down a little and ESDs are also removed for larger time. In the case of atom A-field b, we do not see any noticeable change in the dynamics. However, for the field a-field b subsystem, the amplitude increases further and no ESD is observed. For $J_z = 1.0$, small peaks in the dynamics of $C(t)$ appear earlier in the dynamics and its height increases with time while the initial peak decreases. As a result the duration of the ESDs gets smaller. For other subsystems, $N(t)$ follow the dynamics for $J_z = 0.7$ with decreased peak height for atom A-field a entanglement while increased peak height for atom A-field b and field a-field b subsystems.

The effects of Ising interaction on entanglements in DCJM are depicted in Fig. 11. In this case also, we observe that for small values of J_z (0.1 and 0.3), $C(t)$ and $N(t)$ for all the subsystems do not change considerably. Only field-field entanglement increases slightly for $J_z = 0.3$. For $J_z = 0.7$, length of ESD for $C(t)$ increase slightly as the small bump disappears from the dynamics. The amplitudes atom-field entanglement do change noticeably, however the length of ESD decreases for atom A-field b entanglement. For $J_z = 1.0$, two small peaks appear in the dynamics of $C(t)$ which makes the length of ESDs smaller. All the other entanglement dynamics remain almost unchanged. So, we see that Ising interaction is not much effective to remove sudden death of entanglement for atom-atom subsystem and also from the atom A-field b subsystem.

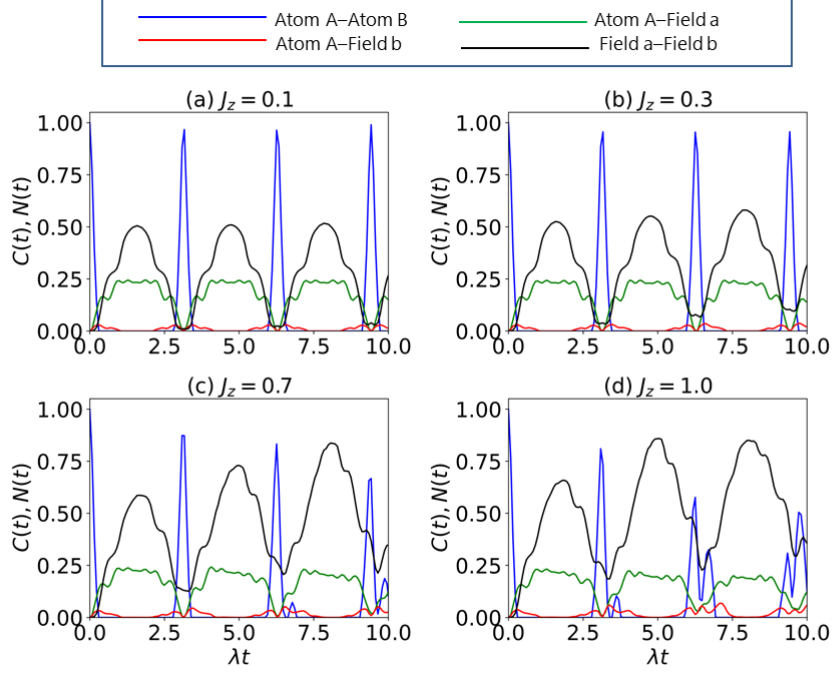


Figure 10: Effects of Ising interaction on entanglement dynamics in IDDJCM. The values of the parameters used in these plots are $\bar{n}_c = 2$, $\bar{n}_{th} = 0.1$, $\bar{n}_s = 1.0$, $J_z = 0.1, 0.3, 0.7, 1.0$ and $\theta = \frac{\pi}{4}$.

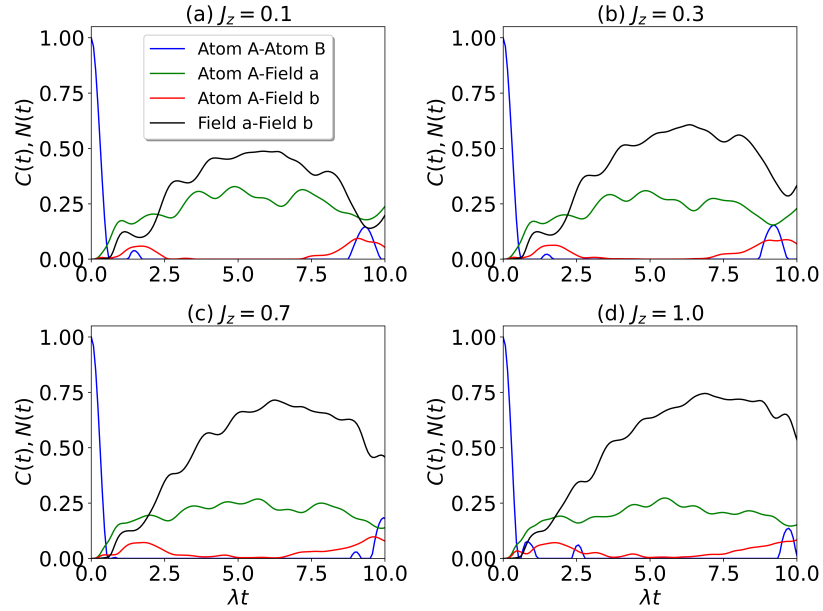


Figure 11: Effects of Ising interaction on entanglement dynamics in DJCM. The values of the parameters used in these plots are $\bar{n}_c = 2$, $\bar{n}_{th} = 0.1$, $\bar{n}_s = 1.0$, $J_z = 0.1, 0.3, 0.7, 1.0$ and $\theta = \frac{\pi}{4}$.

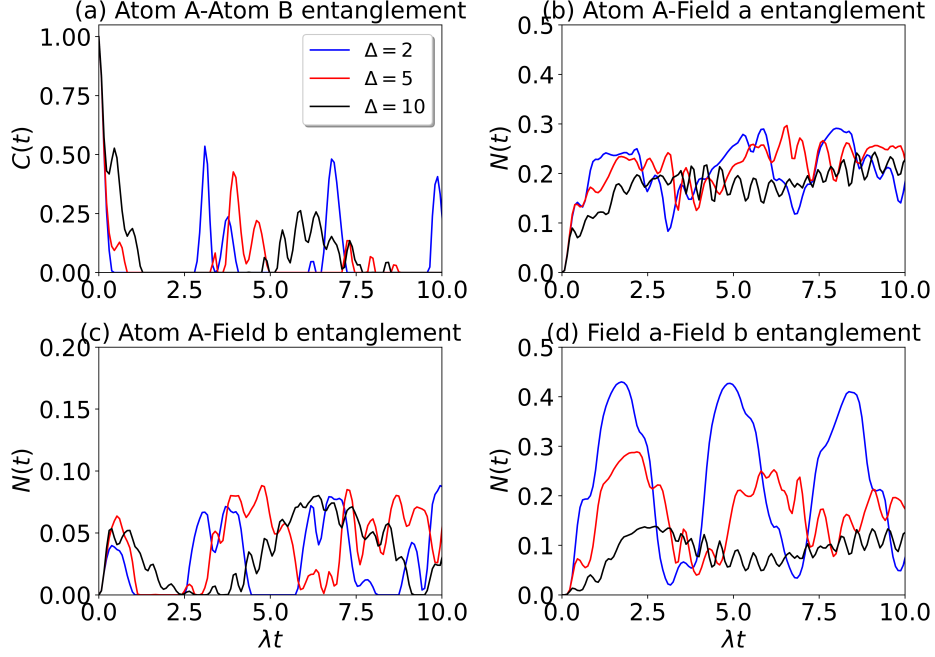


Figure 12: Effects of detuning on entanglement dynamics for SCTS in IDDJCM. The values of the parameters used in these plots are $\bar{n}_c = 2$, $\bar{n}_{th} = 0.1$, $\bar{n}_s = 1.0$, $\Delta = 2, 5, 10$ and $\theta = \frac{\pi}{4}$.

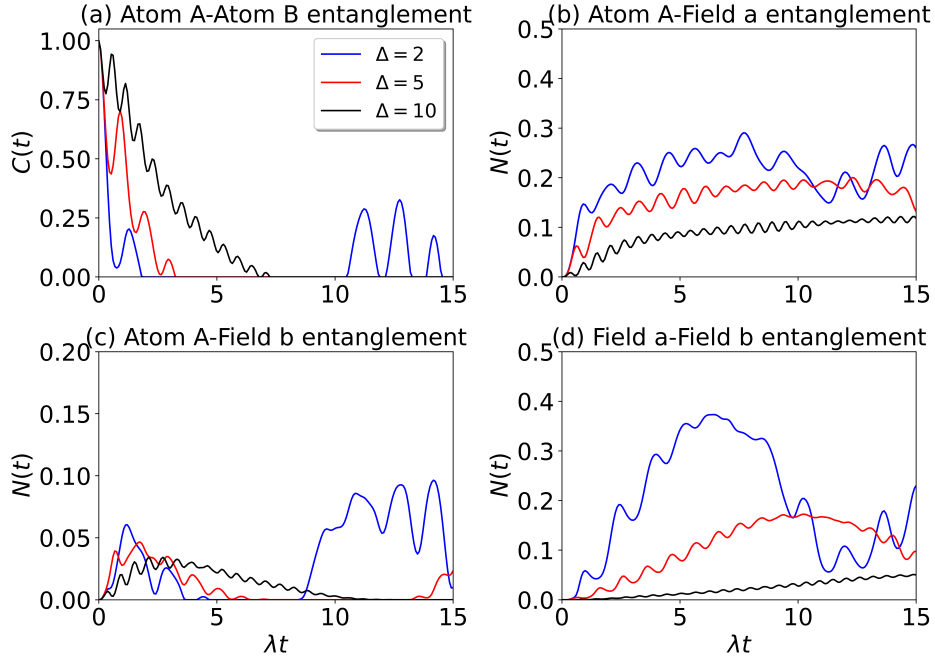


Figure 13: Effects of detuning on entanglement dynamics for SCTS in DJCM. The values of the parameters used in these plots are $\bar{n}_c = 2$, $\bar{n}_{th} = 0.1$, $\bar{n}_s = 1.0$, $\Delta = 2, 5, 10$ and $\theta = \frac{\pi}{4}$.

7 Effects of detuning on the entanglement dynamics for SCTS in and IDDJCM and DJCM

Now, we discuss the effects of detuning on the entanglement dynamics of various subsystems. Detuning is defined as $\Delta = \omega - \nu$. In various studies, the effects of detuning on the dynamics of atom-field interaction have been investigated. The Hamiltonian of the atom-field system after adding detuning becomes

$$\hat{H}_{\text{det}} = \Delta \hat{\sigma}_-^A \hat{\sigma}_+^A + \lambda(\hat{a}^\dagger \hat{\sigma}_-^A + \hat{a} \hat{\sigma}_+^A) + \Delta \hat{\sigma}_-^B \hat{\sigma}_+^B + \lambda(\hat{b}^\dagger \hat{\sigma}_-^B + \hat{b} \hat{\sigma}_+^B), \quad (48)$$

$$\hat{H}'_{\text{det}} = \Delta \hat{\sigma}_-^A \hat{\sigma}_+^A + \lambda \left(\sqrt{\hat{N}_a} \hat{a}^\dagger \hat{\sigma}_-^A + \hat{a} \sqrt{\hat{N}_a} \hat{\sigma}_+^A \right) + \Delta \hat{\sigma}_-^B \hat{\sigma}_+^B + \lambda \left(\sqrt{\hat{N}_b} \hat{b}^\dagger \hat{\sigma}_-^B + \hat{b} \sqrt{\hat{N}_b} \hat{\sigma}_+^B \right). \quad (49)$$

To study the effects of detuning $\bar{n}_c = 2, \bar{n}_s = 1.0$ and $\bar{n}_{th} = 0.1$ are chosen while the values of Δ are taken to be 2, 5, 10. The effects of detuning on entanglements for SCTS in IDDJCM is plotted in Fig. 12. From the plots it is very much noticeable that Δ plays a significant role in removing ESDs from the system. For $\Delta = 2$, length of ESDs get decreased in the dynamics of $C(t)$ (blue curve in Fig. 12(a)) by introducing new smaller peaks in the dynamics. Another important fact is that the detuning decreases the peak heights of the entanglement pulses significantly with increasing time; however the periodic nature of $C(t)$ is present to some extent. For atom A-field a entanglement, we see that the addition of Δ in the system totally destroys the periodic nature of the dynamics of $N(t)$. The amplitude of $N(t)$ is increased and all the ESDs are removed from the dynamics. The periodic pulse like nature of $N(t)$ for atom A-field b is also get destroyed by the addition of Δ in the system. For this smaller value of Δ , length of the ESDs get smaller however these are not removed from the dynamics. In the case of field a-field b subsystem it is observed that the addition of $\Delta = 2$ removes all the ESDs from the dynamics of $N(t)$. Although, the periodic nature of $N(t)$ is present in the dynamics, the form of the periodic nature of is distorted significantly.

For $\Delta = 5$, the height of the peaks of $C(t)$ comes down further with smaller peaks appearing in some places of the dynamics. This makes the length of ESDs larger at some places and smaller at some places. Also the entanglement pulses are destroyed with increasing Δ . $N(t)$ for atom A-field a does not change considerably, while for atom A-field b the amplitude of $N(t)$ increases and some of the ESDs get removed from the dynamics. For field a-field b subsystems, it is observed that the amplitude of $N(t)$ becomes almost half of the initial peak and the periodicity of the dynamics is totally lost.

As Δ is increased to $\Delta = 10$, the length of initial ESD increases as a result of disappearance of other peaks from the dynamics. The dynamics becomes oscillatory for a short time and again ESDs appear. So, we can see that detuning is not much effective to remove the ESDs from the dynamics of $C(t)$ and increases the value of atom-atom entanglement which is observed for SCS and G-L states.

The effects of Δ for SCTS in DJCM is depicted in Fig. 13. For $\Delta = 2$, initial ESD is removed from the dynamics of $C(t)$, however the peak after the second long ESD is lost (see black curve in Fig. 3(a) and blue curve in Fig. 13(a)), which makes the second ESD even longer. For the all the other subsystems, the addition of Δ decreases the amplitude $N(t)$. For the higher values of $\Delta = 5, 10$, though the amplitude of $C(t)$ increases more initially, the length of later ESDs increases significantly. In the case of other subsystems, $N(t)$ is decreased further which makes ESD appear initially in field-field entanglement. From these plots it is evident that presence of thermal photons bar entanglement transfer to atom-atom subsystem from other subsystems.

8 Effects of dipole-dipole interaction between the two atoms

In this section, the effects of dipole-dipole interaction on entanglement dynamics are discussed. The intensity-dependent double JC Hamiltonian with dipole-dipole interaction can be written as

$$\hat{H}_{\text{dd}} = \hat{H} + g_d(\hat{\sigma}_+^A \hat{\sigma}_-^B + \hat{\sigma}_-^A \hat{\sigma}_+^B), \quad (50)$$

where g_d is the dipole-dipole coupling strength. For the double Jaynes-Cummings model, this Hamiltonian becomes

$$\hat{H}'_{\text{dd}} = \hat{H}' + g_d(\hat{\sigma}_+^A \hat{\sigma}_-^B + \hat{\sigma}_-^A \hat{\sigma}_+^B). \quad (51)$$

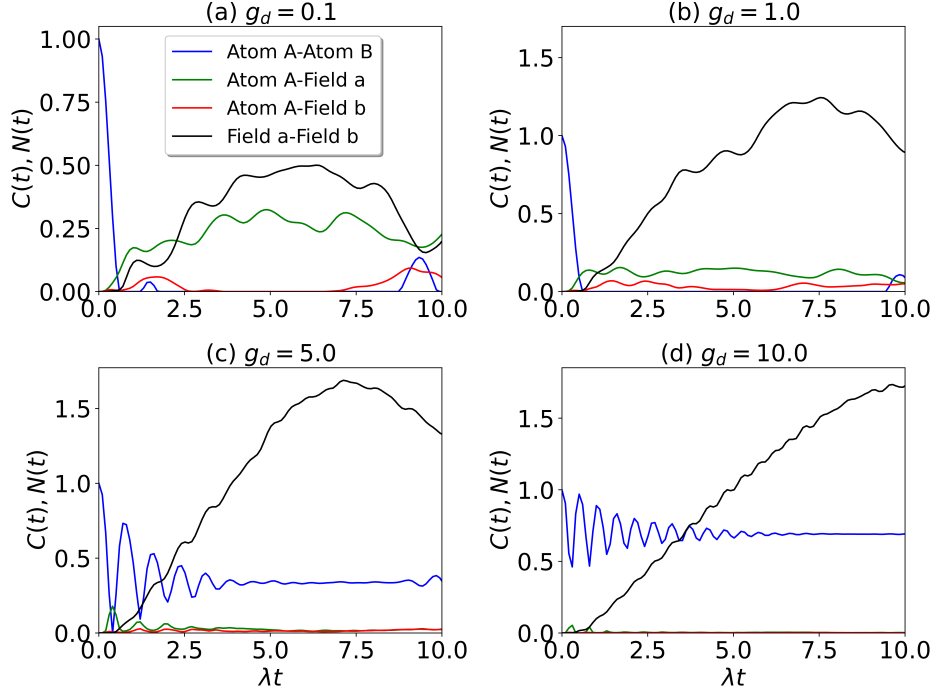


Figure 14: Effects of dipole-dipole interaction for SCTS in IDDJCM. The values of the parameters used in these plots are $\bar{n}_c = 2$, $\bar{n}_{th} = 0.1$, $\bar{n}_s = 1.0$, $g_d = 0.1, 1.0, 5.0, 10.0$ and $\theta = \frac{\pi}{4}$.

People have shown interest in studying the effects of the dipole-dipole interaction on the dynamics of the atom-field system for a long time. In particular, the authors in [81], have discussed a detailed dynamics of the two-atom system where two atoms are interacting with each other via dipole-dipole coupling. A remarkable feature which comes out of this study is that more series of revivals appear in the dynamics that are like the one-atom case, partial and overlapping. They have also found that quantum collapse is no longer Gaussian and now depends on the dipole-dipole interaction parameter. In ref. [82], Evseev *et al.*, have investigated entanglement dynamics between two qubits in a non-resonant DJCM taking into account the direct dipole-dipole interaction between the qubits. The results show that the dipole-dipole parameter has great impact on the entanglement dynamics. They have also shown that the presence of large g_d leads to a stabilization of entanglement for all Bell-types initial qubit states and different couplings and detunings. In another paper [83] the authors have studied the nonlinear version of the Jaynes-Cummings model for two identical two-level atoms for Ising-like and dipole-dipole interaction between the atoms. They have found that when the ratio of $\frac{g_d - J_z}{\lambda} \gg 1$, some significant results are observed. The effects of dipole-dipole interaction on the energy levels of an one dimensional system using Jaynes-Cummings Hubbard model is discussed in ref. [84].

The effects of the dipole-dipole interaction on entanglement dynamics for the IDDJCM is represented in Fig. 14. From Fig. 14(a), it can be seen that all the dynamics almost remain unchanged for $g_d = 0.1$. Only field-field entanglement rises up for larger time making ESDs disappear. For $g_d = 1.0$, peaks of $C(t)$ come down remarkably but length of ESDs remains same. The field-field entanglement increases more and all the ESDs are removed from the dynamics. The amplitude of $N(t)$ for atom A-field a comes down however, $N(t)$ for the atom A-field b does not change considerably. For $g_d = 5$, it is observed that new peaks start to appear in the dynamics of $C(t)$ and all the ESDs are removed the dynamics for $g_d = 10$. The field-field entanglement remains high as before. However, the atom-field entanglements almost becomes zero for $g_d = 10$.

The effects of dipole-dipole interaction for DJCM with SCTS is plotted in Fig. 15. The effects for $g_d = 0.1$ and $g_d = 1.0$ are almost similar as we observe in photon exchange interaction for $\kappa = 0.1$ and 1.0 . For $g_d = 5$, we observe that field-field entanglement is different from the dynamics for $\kappa = 5$. In this case no oscillation is found in the dynamics though its amplitude increases significantly. The behaviour of other entanglements are quite similar. When g_d is increased to 10, all the ESDs are removed from the dynamics of $C(t)$. Also the amplitude of oscillations are increased; however the oscillations die after

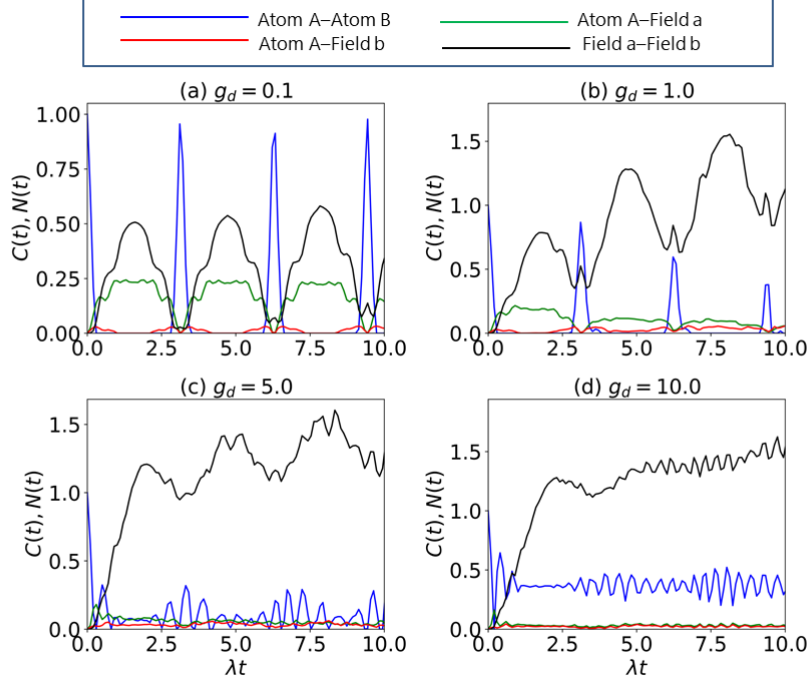


Figure 15: Effects of dipole-dipole interaction on entanglement dynamics for SCTS in DJCM. The values of the parameters used in these plots are $\bar{n}_c = 2$, $\bar{n}_{th} = 0.1$, $\bar{n}_s = 1.0$, $g_d = 0.1, 1.0, 5.0, 10.0$ and $\theta = \frac{\pi}{4}$.

sometime. For the field-field entanglement, it is noticed that the downward fall of the dynamics stops. The atom-field entanglements become zero for this high value of dipole-dipole interaction.

9 Conclusion

In this work we have investigated the entanglement dynamics of the atom-atom, atom-field and field-field subsystems with squeezed coherent thermal states in intensity-dependent double Jaynes-Cummings model (IDDJCM) and double Jaynes-Cummings model (DJCM). It is noticed that the atom-atom and field-field entanglements almost remain unchanged with increasing number of squeezed photons while keeping coherent and thermal photons constant for IDDJCM. An array of entanglement pulses is formed with almost same ESDs and same peak amplitude. However, the atom-field entanglements are affected noticeably. For DJCM, all the dynamics change with increasing squeezed photons and length of ESDs also increases for atom-atom and atom A-field b subsystems.

The addition of photon exchange interaction between the cavities removes ESDs from field-field entanglement dynamics and from the atom-atom for large values of κ for both IDDJCM and DJCM. The atom-field entanglements become zero for large values of κ . In the case of DJCM, formation of wave packets is observed for field-field subsystem. Kerr-nonlinearity effectively removes ESDs from the all the entanglement dynamics. For IDDJCM, $C(t)$ and $N(t)$ for all the subsystems increase for higher values of χ . In the case of DJCM also, $C(t)$ and $N(t)$ for atom-field subsystems increase for higher values of χ , however, field-field entanglement decreases after a critical value of χ .

Ising interaction is effective to remove ESDs from field-field entanglement for IDDJCM; however, it is unable to remove ESDs from atom-atom and atom-field entanglements. For DJCM, the dynamics of $C(t)$ and $N(t)$ are not affected considerably by the addition of Ising interaction in the system. Detuning tries to remove ESDs from all the subsystems. ESDs are removed from field-field entanglement, however its amplitude comes down with increasing value of Δ . Also, for higher values of detuning, the $C(t)$ increases more and other entanglements decreases which is a implications of entanglement transfer from other subsystems to atom-atom subsystems. Like photon exchange interaction, dipole-dipole interaction removes ESDs from the dynamics of $C(t)$ and $N(t)$ of field-field subsystem for high value of g_d for both IDDJCM and DJCM. However, in this case, wave packets formation is observed.

Acknowledgements

The author thanks Prof. M. V. Satyanarayana for all the valuable discussions and suggestions.

References

- [1] Horodecki, R., Horodecki, P., Horodecki, M. & Horodecki, K. Quantum entanglement. *Rev. Mod. Phys.* **81**, 865–942 (2009). URL <https://link.aps.org/doi/10.1103/RevModPhys.81.865>.
- [2] Bennett, C. H. *et al.* Teleporting an unknown quantum state via dual classical and einstein-podolsky-rosen channels. *Phys. Rev. Lett.* **70**, 1895–1899 (1993). URL <https://link.aps.org/doi/10.1103/PhysRevLett.70.1895>.
- [3] Bennett, C. H. & Wiesner, S. J. Communication via one- and two-particle operators on einstein-podolsky-rosen states. *Phys. Rev. Lett.* **69**, 2881–2884 (1992). URL <https://link.aps.org/doi/10.1103/PhysRevLett.69.2881>.
- [4] Bermudez, A., Martin-Delgado, M. A. & Solano, E. Exact mapping of the $2 + 1$ dirac oscillator onto the jaynes-cummings model: Ion-trap experimental proposal. *Phys. Rev. A* **76**, 041801 (2007). URL <https://link.aps.org/doi/10.1103/PhysRevA.76.041801>.
- [5] Lv, D. *et al.* Reconstruction of the jaynes-cummings field state of ionic motion in a harmonic trap. *Phys. Rev. A* **95**, 043813 (2017). URL <https://link.aps.org/doi/10.1103/PhysRevA.95.043813>.
- [6] Krumm, F. & Vogel, W. Time-dependent nonlinear jaynes-cummings dynamics of a trapped ion. *Phys. Rev. A* **97**, 043806 (2018). URL <https://link.aps.org/doi/10.1103/PhysRevA.97.043806>.
- [7] Cirac, J., Parkins, A., Blatt, R. & Zoller, P. Nonclassical states of motion in ion traps a version of this chapter has been submitted to advances of atomic and molecular physics. vol. 37 of *Advances In Atomic, Molecular, and Optical Physics*, 237–296 (Academic Press, 1996). URL <https://www.sciencedirect.com/science/article/pii/S1049250X08601020>.
- [8] Guerlin, C., Brion, E., Esslinger, T. & Mølmer, K. Cavity quantum electrodynamics with a rydberg-blocked atomic ensemble. *Phys. Rev. A* **82**, 053832 (2010). URL <https://link.aps.org/doi/10.1103/PhysRevA.82.053832>.
- [9] W. Rosado, F. P., G.D. de Moraes Neto & Moussa, M. Upper bounded and sliced jaynes- and anti-jaynes-cummings hamiltonians and liouvillians in cavity quantum electrodynamics. *Journal of Modern Optics* **62**, 1561–1569 (2015). URL <https://doi.org/10.1080/09500340.2015.1051150>.
- [10] Ahmadi, E., Chalabi, H., Arab, A. & Khorasani, S. Cavity quantum electrodynamics in the ultrastrong coupling regime. *Scientia Iranica* **18**, 820–826 (2011). URL <https://www.sciencedirect.com/science/article/pii/S1026309811001143>.
- [11] Niemczyk, T. *et al.* Circuit quantum electrodynamics in the ultrastrong-coupling regime. *Nature Physics* **6**, 772–776 (2010). URL <https://doi.org/10.1038/nphys1730>.
- [12] Haroche, S., Brune, M. & Raimond, J. From cavity to circuit quantum electrodynamics. *Nature Physics* **16**, 243–246 (2020). URL <https://doi.org/10.1038/s41567-020-0812-1>.
- [13] Fink, J. *et al.* Climbing the jaynes-cummings ladder and observing its nonlinearity in a cavity qed system. *Nature* **454**, 315–318 (2008). URL <https://doi.org/10.1038/nature07112>.
- [14] Reed, M. D. *et al.* High-fidelity readout in circuit quantum electrodynamics using the jaynes-cummings nonlinearity. *Phys. Rev. Lett.* **105**, 173601 (2010). URL <https://link.aps.org/doi/10.1103/PhysRevLett.105.173601>.
- [15] Bradford, M. & Shen, J.-T. Architecture dependence of photon antibunching in cavity quantum electrodynamics. *Phys. Rev. A* **92**, 023810 (2015). URL <https://link.aps.org/doi/10.1103/PhysRevA.92.023810>.

- [16] Mamgain, A., Hawaldar, S., Shankar, A. & Suri, B. Characterizing polariton states in the nondispersive regime of circuit quantum electrodynamics. *Physical Review A* **108** (2023). URL <http://dx.doi.org/10.1103/PhysRevA.108.033703>.
- [17] PERSSON, D. L. Hybrid microwave resonator-nanoscale conductor systems (2023). URL <https://lup.lub.lu.se/luur/download?func=downloadFile&recordId=9111371&fileId=9111373>.
- [18] Yonac, M., Yu, T. & Eberly, J. Sudden death of entanglement of two jaynes-cummings atoms. *Journal of Physics B Atomic Molecular and Optical Physics* **39** (2006). URL <https://www.researchgate.net/publication/2197779>.
- [19] Yönaç, M., Yu, T. & Eberly, J. H. Sudden death of entanglement of two jaynes-cummings atoms. *Journal of Physics B: Atomic, Molecular and Optical Physics* **39**, S621 (2006). URL <https://dx.doi.org/10.1088/0953-4075/39/15/S09>.
- [20] Yu, T. & Eberly, J. H. Quantum open system theory: Bipartite aspects. *Phys. Rev. Lett.* **97**, 140403 (2006). URL <https://link.aps.org/doi/10.1103/PhysRevLett.97.140403>.
- [21] Yu, T. & Eberly, J. H. Sudden death of entanglement. *Science* **323**, 598–601 (2009). URL <https://www.science.org/doi/abs/10.1126/science.1167343>. <https://www.science.org/doi/pdf/10.1126/science.1167343>.
- [22] Yu, T. & Eberly, J. Sudden death of entanglement: Classical noise effects. *Optics Communications* **264**, 393–397 (2006). URL <https://www.sciencedirect.com/science/article/pii/S0030401806005104>. Quantum Control of Light and Matter.
- [23] Yönaç, M., Yu, T. & Eberly, J. H. Pairwise concurrence dynamics: a four-qubit model. *Journal of Physics B: Atomic, Molecular and Optical Physics* **40**, S45 (2007). URL <https://dx.doi.org/10.1088/0953-4075/40/9/S02>.
- [24] Yu, T. & Eberly, J. Evolution from entanglement to decoherence of bipartite mixed” x” states. *arXiv preprint quant-ph/0503089* (2005). URL <https://doi.org/10.48550/arXiv.quant-ph/0503089>.
- [25] Yu, T. & Eberly, J. Sudden death of entanglement. *Science* **323**, 598–601 (2009). URL <https://www.science.org/doi/full/10.1126/science.1167343>.
- [26] Eberly, J. H. & Yu, T. The end of an entanglement. *Science* **316**, 555–557 (2007). URL <https://www.science.org/doi/abs/10.1126/science.1142654>. <https://www.science.org/doi/pdf/10.1126/science.1142654>.
- [27] Sainz, I. & Björk, G. Entanglement invariant for the double jaynes-cummings model. *Phys. Rev. A* **76**, 042313 (2007). URL <https://link.aps.org/doi/10.1103/PhysRevA.76.042313>.
- [28] Pandit, M., Das, S., Roy, S. S., Dhar, H. S. & Sen, U. Effects of cavity-cavity interaction on the entanglement dynamics of a generalized double jaynes-cummings model. *Journal of Physics B: Atomic, Molecular and Optical Physics* **51**, 045501 (2018). URL <https://doi.org/10.1088/1361-6455/aaa2cf>.
- [29] Li, Z.-j., Zhang, J., Hu, P. & Han, Z.-w. Entanglement dynamics of two atoms in the squeezed vacuum and the coherent fields. *International Journal of Theoretical Physics* **59**, 730–742 (2020). URL <https://doi.org/10.1007/s10773-019-04359-2>.
- [30] Jakubczyk, P., Majchrowski, K. & Tralle, I. Quantum entanglement in double quantum systems and jaynes-cummings model. *Nanoscale research letters* **12**, 1–9 (2017). URL <https://doi.org/10.1186/s11671-017-1985-0>.
- [31] Ghoshal, A., Das, S., Sen(De), A. & Sen, U. Population inversion and entanglement in single and double glassy jaynes-cummings models. *Phys. Rev. A* **101**, 053805 (2020). URL <https://link.aps.org/doi/10.1103/PhysRevA.101.053805>.
- [32] Obada, A.-S. F., Khalil, E., Ahmed, M. & Elmalky, M. Influence of an external classical field on the interaction between a field and an atom in presence of intrinsic damping. *International Journal of Theoretical Physics* **57**, 2787–2801 (2018). URL <https://doi.org/10.1007/s10773-018-3799-y>.
- [33] Laha, P. Dynamics of a multipartite hybrid quantum system with beamsplitter, dipole-dipole. *Journal of the Optical Society of America B* **7**, 1–2 (2023). URL <https://doi.org/10.1364/JOSAB.489223>.

- [34] Faghihi, M. J. & Tavassoly, M. K. Quantum entanglement and position–momentum entropic squeezing of a moving lambda-type three-level atom interacting with a single-mode quantized field with intensity-dependent coupling. *Journal of Physics B: Atomic, Molecular and Optical Physics* **46**, 145506 (2013). URL <https://dx.doi.org/10.1088/0953-4075/46/14/145506>.
- [35] and and. Entropy squeezing and atomic inversion in the k-photon jaynes–cummings model in the presence of the stark shift and a kerr medium: A full nonlinear approach. *Chinese Physics B* **23**, 074203 (2014). URL <https://dx.doi.org/10.1088/1674-1056/23/7/074203>.
- [36] Bužek, V. Light squeezing in the jaynes-cummings model with intensity-dependent coupling. *Journal of Modern Optics* **36**, 1151–1162 (1989). URL <https://doi.org/10.1080/09500348914551181>.
- [37] Bužek, V. Jaynes-cummings model with intensity-dependent coupling interacting with holstein-primakoff su(1,1) coherent state. *Phys. Rev. A* **39**, 3196–3199 (1989). URL <https://link.aps.org/doi/10.1103/PhysRevA.39.3196>.
- [38] Buzek, V. & Jex, I. Emission spectra for the jaynes-cummings model with intensity-dependent coupling. *Quantum Optics: Journal of the European Optical Society Part B* **2**, 147 (1990). URL <https://dx.doi.org/10.1088/0954-8998/2/2/005>.
- [39] Naderi, M. H. The jaynes–cummings model beyond the rotating-wave approximation as an intensity-dependent model: quantum statistical and phase properties. *Journal of Physics A: Mathematical and Theoretical* **44**, 055304 (2011). URL <https://dx.doi.org/10.1088/1751-8113/44/5/055304>.
- [40] Naderi, M., Soltanolkotiabi, M. & Rognizadeh, R. A theoretical scheme for generation of nonlinear coherent states in a micromaser under intensity-dependent jaynes-cummings model. *The European Physical Journal D-Atomic, Molecular, Optical and Plasma Physics* **32**, 397–408 (2005). URL <https://doi.org/10.1140/epjd/e2004-00197-8>.
- [41] Lo, C., Liu, K. & Ng, K. The multiquantum intensity-dependent jaynes–cummings model with the counterrotating terms. *Physica A: Statistical Mechanics and its Applications* **265**, 557–564 (1999). URL <https://www.sciencedirect.com/science/article/pii/S0378437198006499>.
- [42] Ng, K., Lo, C. & Liu, K. Exact eigenstates of the intensity-dependent jaynes–cummings model with the counter-rotating term. *Physica A: Statistical Mechanics and its Applications* **275**, 463–474 (2000). URL <https://www.sciencedirect.com/science/article/pii/S037843719900401X>.
- [43] Qin, X. & Mao-Fa, F. Entanglement dynamics of the double intensity-dependent coupling jaynes-cummings models. *International Journal of Theoretical Physics* **51**, 778–786 (2012). URL <https://doi.org/10.1007/s10773-011-0957-x>.
- [44] Góra, P. & Jędrzejek, C. Nonlinear jaynes-cummings model. *Phys. Rev. A* **45**, 6816–6828 (1992). URL <https://link.aps.org/doi/10.1103/PhysRevA.45.6816>.
- [45] Joshi, A. & Puri, R. R. Dynamical evolution of the two-photon jaynes-cummings model in a kerr-like medium. *Phys. Rev. A* **45**, 5056–5060 (1992). URL <https://link.aps.org/doi/10.1103/PhysRevA.45.5056>.
- [46] Werner, M. J. & Risken, H. Quasiprobability distributions for the cavity-damped jaynes-cummings model with an additional kerr medium. *Phys. Rev. A* **44**, 4623–4632 (1991). URL <https://link.aps.org/doi/10.1103/PhysRevA.44.4623>.
- [47] Ahmed, A. & Sivakumar, S. Dynamics of entanglement in a two-mode nonlinear jaynes-cummings mode. *arXiv preprint arXiv:0907.2992* (2009). URL <https://doi.org/10.48550/arXiv.0907.2992>.
- [48] Sivakumar, S. Nonlinear jaynes–cummings model of atom–field interaction. *International Journal of Theoretical Physics* **43**, 2405–2421 (2004). URL <https://doi.org/10.1007/s10773-004-7707-2>.
- [49] Mo, C., Xu, K. & Zhang, G.-F. The entanglement and second-order coherence function in a two-atom nonlinear jaynes-cummings model. *Physica Scripta* **97**, 035101 (2022). URL <https://dx.doi.org/10.1088/1402-4896/ac4cfe>.
- [50] Xiong, W., Tian, M., Zhang, G.-Q. & You, J. Q. Strong long-range spin-spin coupling via a kerr magnon interface. *Phys. Rev. B* **105**, 245310 (2022). URL <https://link.aps.org/doi/10.1103/PhysRevB.105.245310>.

- [51] Zheng, L. & Zhang, G.-F. Intrinsic decoherence in jaynes-cummings model with heisenberg exchange interaction. *The European Physical Journal D* **71**, 1–4 (2017). URL <https://doi.org/10.1140/epjd/e2017-80408-y>.
- [52] Xiong, W., Jin, D.-Y., Qiu, Y., Lam, C.-H. & You, J. Q. Cross-kerr effect on an optomechanical system. *Phys. Rev. A* **93**, 023844 (2016). URL <https://link.aps.org/doi/10.1103/PhysRevA.93.023844>.
- [53] Baghshahi, H., Tavassoly, M. & Faghihi, M. Entanglement analysis of a two-atom nonlinear jaynes-cummings model with nondegenerate two-photon transition, kerr nonlinearity, and two-mode stark shift. *Laser Physics* **24**, 125203 (2014). URL <https://dx.doi.org/10.1088/1054-660X/24/12/125203>.
- [54] Faghihi, M. J. & Tavassoly, M. K. Number-phase entropic squeezing and nonclassical properties of a three-level atom interacting with a two-mode field: intensity-dependent coupling, deformed kerr medium, and detuning effects. *J. Opt. Soc. Am. B* **30**, 2810–2818 (2013). URL <https://opg.optica.org/josab/abstract.cfm?URI=josab-30-11-2810>.
- [55] Baghshahi, H., Tavassoly, M. K. & Akhtarshenas, S. J. Generation and nonclassicality of entangled states via the interaction of two three-level atoms with a quantized cavity field assisted by a driving external classical field. *Quantum Information Processing* **14**, 1279–1303 (2015). URL <https://doi.org/10.1007/s11128-015-0915-2>.
- [56] Mandal, K. & Satyanarayana, M. Atomic inversion and entanglement dynamics for squeezed coherent thermal states in the jaynes-cummings model. *International Journal of Theoretical Physics* **62**, 1–19 (2023). URL <https://doi.org/10.1007/s10773-023-05389-7>.
- [57] Marian, P. & Marian, T. A. Squeezed states with thermal noise. i. photon-number statistics. *Phys. Rev. A* **47**, 4474–4486 (1993). URL <https://link.aps.org/doi/10.1103/PhysRevA.47.4474>.
- [58] Marian, P. & Marian, T. A. Squeezed states with thermal noise. ii. damping and photon counting. *Phys. Rev. A* **47**, 4487–4495 (1993). URL <https://link.aps.org/doi/10.1103/PhysRevA.47.4487>.
- [59] Yi-min, L., Hui-rong, X., Zu-geng, W. & Zai-xin, X. Squeezed coherent thermal state and its photon number distribution. *Acta Physica Sinica (Overseas Edition)* **6**, 681 (1997). URL <https://doi.org/10.1088/1004-423x/6/9/006>.
- [60] Glauber, R. J. Coherent and incoherent states of the radiation field. *Phys. Rev.* **131**, 2766–2788 (1963). URL <https://link.aps.org/doi/10.1103/PhysRev.131.2766>.
- [61] Wootters, W. K. Entanglement of formation and concurrence. *Quantum Inf. Comput.* **1**, 27–44 (2001). URL <https://arxiv.org/pdf/quant-ph/9709029>.
- [62] Wei, T.-C. *et al.* Maximal entanglement versus entropy for mixed quantum states. *Physical Review A* **67**, 022110 (2003). URL <https://link.aps.org/doi/10.1103/PhysRevA.67.022110>.
- [63] Chaturvedi, S. & Srinivasan, V. Photon-number distributions for fields with gaussian wigner functions. *Phys. Rev. A* **40**, 6095–6098 (1989). URL <https://link.aps.org/doi/10.1103/PhysRevA.40.6095>.
- [64] Janszky, J. & Yushin, Y. Many-photon processes with the participation of squeezed light. *Phys. Rev. A* **36**, 1288–1292 (1987). URL <https://link.aps.org/doi/10.1103/PhysRevA.36.1288>.
- [65] Vourdas, A. Superposition of squeezed coherent states with thermal light. *Phys. Rev. A* **34**, 3466–3469 (1986). URL <https://link.aps.org/doi/10.1103/PhysRevA.34.3466>.
- [66] Ezawa, H., Mann, A., Nakamura, K. & Revzen, M. Characterization of thermal coherent and thermal squeezed states. *Annals of Physics* **209**, 216–230 (1991). URL <https://www.sciencedirect.com/science/article/pii/000349169190360K>.
- [67] Kim, M. S., de Oliveira, F. A. M. & Knight, P. L. Properties of squeezed number states and squeezed thermal states. *Phys. Rev. A* **40**, 2494–2503 (1989). URL <https://link.aps.org/doi/10.1103/PhysRevA.40.2494>.
- [68] Yamamoto, Y. & Haus, H. A. Preparation, measurement and information capacity of optical quantum states. *Rev. Mod. Phys.* **58**, 1001–1020 (1986). URL <https://link.aps.org/doi/10.1103/RevModPhys.58.1001>.

- [69] Kitagawa, M. & Ueda, M. Squeezed spin states. *Phys. Rev. A* **47**, 5138–5143 (1993). URL <https://link.aps.org/doi/10.1103/PhysRevA.47.5138>.
- [70] Ralph, T. C. Continuous variable quantum cryptography. *Phys. Rev. A* **61**, 010303 (1999). URL <https://link.aps.org/doi/10.1103/PhysRevA.61.010303>.
- [71] Hillery, M. Quantum cryptography with squeezed states. *Phys. Rev. A* **61**, 022309 (2000). URL <https://link.aps.org/doi/10.1103/PhysRevA.61.022309>.
- [72] Braunstein, S. L. & Kimble, H. J. Teleportation of continuous quantum variables. *Phys. Rev. Lett.* **80**, 869–872 (1998). URL <https://link.aps.org/doi/10.1103/PhysRevLett.80.869>.
- [73] Milburn, G. J. & Braunstein, S. L. Quantum teleportation with squeezed vacuum states. *Phys. Rev. A* **60**, 937–942 (1999). URL <https://link.aps.org/doi/10.1103/PhysRevA.60.937>.
- [74] Hillery, M., O’Connell, R., Scully, M. & Wigner, E. Distribution functions in physics: Fundamentals. *Physics Reports* **106**, 121–167 (1984). URL <https://www.sciencedirect.com/science/article/pii/0370157384901601>.
- [75] Schleich, W. P. *Quantum Optics in Phase Space* (Wiley-VCH, 2001).
- [76] Agarwal, G. S. *Quantum Optics* (Cambridge University Press, 2013).
- [77] Mojaveri, B., Dehghani, A., Fasihi, M. & Mohammadpour, T. Thermal entanglement between two two-level atoms in a two-photon jaynes-cummings model with an added kerr medium. *International Journal of Theoretical Physics* **57**, 3396–3409 (2018). URL <https://doi.org/10.1007/s10773-018-3853-9>.
- [78] Thabet, L., El-Shahat, T., Abdel-Aty, A. & Rababh, B. Dynamics of entanglement and non-classicality features of a single-mode nonlinear jaynes-cummings model. *Chaos, Solitons & Fractals* **126**, 106–115 (2019). URL <https://www.sciencedirect.com/science/article/pii/S0960077919302036>.
- [79] Hou, X.-W., Chen, J.-H., Wan, M.-F. & Ma, Z.-Q. Linear entropy in the jaynes-cummings model with a kerr nonlinearity. *Optics Communications* **266**, 727–731 (2006). URL <https://www.sciencedirect.com/science/article/pii/S0030401806005505>.
- [80] Sadiq, G., Al-Dress, W., Shaghl, S. & Elhag, H. Asymptotic entanglement sudden death in two atoms with dipole-dipole and ising interactions coupled to a radiation field at non-zero detuning. *Entropy* **23** (2021). URL <https://www.mdpi.com/1099-4300/23/5/629>.
- [81] Joshi, A., Puri, R. R. & Lawande, S. V. Effect of dipole interaction and phase-interrupting collisions on the collapse-and-revival phenomenon in the jaynes-cummings model. *Phys. Rev. A* **44**, 2135–2140 (1991). URL <https://link.aps.org/doi/10.1103/PhysRevA.44.2135>.
- [82] Evseev, M. M. & Bashkirov, E. K. The influence of dipole-dipole interaction on entanglement of two superconducting qubits in the framework of double jaynes-cummins model. *Journal of Physics: Conference Series* **917**, 062011 (2017). URL <https://dx.doi.org/10.1088/1742-6596/917/6/062011>.
- [83] de los Santos-Sánchez, O., González-Gutiérrez, C. & Récamier, J. Nonlinear jaynes-cummings model for two interacting two-level atoms. *Journal of Physics B: Atomic, Molecular and Optical Physics* **49**, 165503 (2016). URL <https://dx.doi.org/10.1088/0953-4075/49/16/165503>.
- [84] Li, Q., Ma, J.-L. & Tan, L. Normal and abnormal thermalization indicators in a one-dimensional low-density jaynes-cummings hubbard model with and without dipole-dipole interaction. *Phys. Rev. E* **106**, 064107 (2022). URL <https://link.aps.org/doi/10.1103/PhysRevE.106.064107>.